Iowa Research Online
The University of Iowa's Institutional Repository

University of Iowa
Iowa Research Online

Theses and Dissertations

Fall 2014

The dosimetric impacts of gated radiation therapy and 4D dose calculation in lung cancer patients

Ouided Rouabhi
University of Iowa

Follow this and additional works at: https://ir.uiowa.edu/etd

 Part of the Biomedical Engineering and Bioengineering Commons

Copyright © 2014 Ouided Rouabhi

This thesis is available at Iowa Research Online: https://ir.uiowa.edu/etd/6631

Recommended Citation

Rouabhi, Ouided. "The dosimetric impacts of gated radiation therapy and 4D dose calculation in lung cancer patients." MS (Master of Science) thesis, University of Iowa, 2014.
https://doi.org/10.17077/etd.dnws-yhjf

Follow this and additional works at: https://ir.uiowa.edu/etd

 Part of the Biomedical Engineering and Bioengineering Commons

www.manaraa.com

THE DOSIMETRIC IMPACTS OF GATED RADIATION THERAPY AND 4D DOSE CALCULATION IN LUNG CANCER PATIENTS

by

Ouided Rouabhi

A thesis submitted in partial fulfillment
of the requirements for the Master of
Science degree in Biomedical Engineering
in the Graduate College of
The University of Iowa

December 2014

Thesis Supervisor: Assistant Professor Junyi Xia

www.manaraa.com

Graduate College
The University of Iowa
Iowa City, Iowa

CERTIFICATE OF APPROVAL

MASTER'S THESIS

This is to certify that the Master's thesis of

Ouided Rouabhi

has been approved by the Examining Committee
for the thesis requirement for the Master of Science degree
in Biomedical Engineering at the December 2014 graduation.

Thesis Committee: _____
Junyi Xia, Thesis Supervisor

_____
Joseph M. Reinhardt

_____
Ryan T. Flynn

www.manaraa.com

ACKNOWLEDGMENTS

I can say without doubt that I have thoroughly enjoyed the pursuit of this degree, and this is in large part due to the extraordinary mentors that I have been fortunate to meet throughout my academic journey. I would first like to thank my thesis supervisor, Dr. Junyi Xia, for allowing me the opportunity to study under his guidance. Without his knowledge, patience, and support, this work would not have been possible. I would also like to thank Dr. Joseph Reinhardt for his academic and professional advising. I truly appreciate your willingness to help and the commitment you have always shown towards your students. Additionally, I would like to express my gratitude towards Dr. Ryan Flynn. Thank you for offering your time and input towards serving as a part of this thesis committee. Finally, I would like to thank my family and friends for their continued encouragement and support.

www.manaraa.com

ABSTRACT

With the introduction of four-dimensional computed tomography (4DCT), treatment centers are now better able to account for respiration-induced uncertainty in radiation therapy treatment planning for lung cancer. We examined two practices in which 4DCT is used in radiotherapy. Our first study investigated the dosimetric uncertainty in four-dimensional (4D) dose calculation using three temporal probability distributions: 1) uniform distribution, 2) sinusoidal distribution, and 3) patient-specific distribution derived from the respiratory trace. Four-dimensional dose was evaluated in nine lung cancer patients. First, dose was computed for each of 10 binned CTs using 4DCT and deformable image registration. Next, the 10 deformed doses were summed together using one of three temporal probability distributions. To compare the two approximated 4D dose calculations to the 4D calculation derived using the patient's respiratory trace, 3D gamma analysis was performed using a tolerance criteria of 3% dose difference and 3mm distance to agreement. Additionally, mean lung dose (MLD), mean tumor dose (MTD), and lung V20 were used to assess clinical impact. For all patients, both uniform and sinusoidal dose distributions were found to have an average gamma passing rate >99% for both the lung and PTV volumes. Compared with 4D dose calculated using the patient respiratory trace, uniform distribution and sinusoidal distribution showed a percentage difference on average of -0.1±0.6% and -0.2±0.4% in MTD, -0.2±2.0% and -0.2±1.3% in MLD, 0.9±2.8% and -0.7±1.8% in lung V20, respectively. We concluded that 4D dose computed using either a uniform or sinusoidal temporal probability distribution is able to approximate 4D dose computed using the patient-specific respiratory trace.

www.manaraa.com

Our second study evaluated the dosimetric and temporal effects of respiratory gated radiation therapy using four different gating windows (20EX-20IN, 40EX-40IN, 60EX-60IN, and 80EX-80IN) and estimated the corresponding treatment delivery times for normal (500MU/min) and high (1500MU/min) dose rates. Five patients (3 non-gated, 2 gated 80EX-80IN) were retrospectively evaluated. For each patient, four individual treatment plans, corresponding to the four different gating windows were created, and treatment delivery time for each plan was estimated using a MATLAB (MathWorks, Natick, MA) algorithm. Results showed that smaller gating windows reduced PTV volume, mean lung dose, and lung V20, while maintaining mean tumor dose and PTV coverage. Treatment times for gated plans were longer when dose rate was unchanged, however, increased dose rates were shown to achieve treatment times comparable to or faster than non-gated delivery times. We concluded that gated radiation therapy in lung cancer patients could potentially reduce lung toxicity, while as effectively treating the target volume. Furthermore, increased dose rates with gated radiation therapy are able to provide treatment times comparable to non-gated treatment.

www.manaraa.com

PUBLIC ABSTRACT

Radiation therapy, a common treatment used for lung cancers, aims to deliver a high dose of radiation to the tumor, while minimizing the amount of radiation received by the surrounding tissues. However, one obstacle remains to be the uncertainty in tumor position caused by the patient's breathing. With the introduction of four-dimensional computed tomography (4DCT), treatment centers are now better able to account for this uncertainty. We examined two practices in which 4DCT is used in radiotherapy. Our first study investigated whether four-dimensional (4D) dose calculation using the patient's respiratory motion could be approximated by 4D calculation using a uniform or sinusoidal respiratory model. Our results showed that differences between the approximated 4D dose calculations and the patient-specific calculation were minimal, leading us to conclude that in the absence of patient respiratory data, 4D dose computed using either a uniform or sinusoidal model is able to approximate 4D dose computed using the patient-specific respiratory trace. Our second study evaluated the effects of respiratory gated radiation therapy. During gated treatment, radiation is only delivered when the patient is within a specific window of the respiratory cycle, thereby reducing the size of the target volume, but consequently, prolonging the time for treatment. Our results showed that gated radiation therapy in lung cancer patients could potentially reduce the radiation dose to healthy lung tissue, while as effectively treating the tumor. Furthermore, increased dose rates with gated radiation therapy are able to provide treatment times comparable to non-gated treatment.

www.manaraa.com

TABLE OF CONTENTS

www.manaraa.com

www.manaraa.com

LIST OF TABLES

Table

www.manaraa.com

www.manaraa.com

LIST OF FIGURES

Figure

www.manaraa.com

www.manaraa.com

www.manaraa.com

CHAPTER 1: INTRODUCTION

The American Cancer Society[1] estimates that more than 224,000 new cases of lung and bronchus cancers will be diagnosed in 2014. For many of these patients, treatment will involve image-guided radiotherapy. Intensity-Modulated Radiation Therapy (IMRT) and Stereotactic Body Radiation Therapy (SBRT) are two treatment modalities commonly employed. These techniques aim to deliver a high dose of radiation to the cancer, while minimizing the radiation dose to healthy tissues [2-5]. One obstacle, however, remains to be the uncertainty in tumor position caused by the patient's respiratory motion. Lung cancers are known to be the most affected site for respiration-induced tumor motion [6]. Studies [7-11] have shown that lung tumors can move more than 10 mm during respiration, with the greatest tumor motion occurring in the lower lobes of the lung. Studies [8, 11, 12] have also shown that the percentage of time spent in each respiratory amplitude is not uniform: patients spend more time in the exhalation phase than in the inhalation phase. In order to ensure correct dose coverage during treatment delivery, the extent of tumor motion within breathing cycles must be evaluated [13].

Conventionally, a free breathing computed tomography (CT)[1] scan has been used for treatment planning [14, 15]. However, tumor motion can introduce severe artifacts, resulting in distortion of the tumor and inaccurate assessment of the tumor's location [16, 17]. By acquiring breath-hold CT scans, motion artifacts may be reduced, however uncertainty in tumor position still remains [14]. In order to compensate for respiration-

[1] Additional resources for computed tomography:
- Prince, J. & Links, J. (2014) *Medical Imaging Signals and Systems*
- Bushberg, J. (2011) *The Essential Physics of Medical Imaging*
- Smith, N., & Webb, A. (2011). *Introduction to Medical Imaging: Physics, Engineering and Clinical Applications*

www.manaraa.com

induced uncertainties in dose distribution, clinicians are often forced to add additional treatment margins to the target volume, resulting in an increased dose to the healthy tissue [15].

With the introduction of four-dimensional computed tomography (4DCT), also known as multiphase CT scanning, treatment centers are now able to better account for respiratory motion. During 4DCT imaging, both the CT projections and the patient's respiratory trace are acquired. The respiratory trace is then used to associate each CT projection with a specific respiratory amplitude, see Figure 1. A binned CT image, also called a phase CT, is then reconstructed for each respiratory amplitude [18-20]. Figure 2 shows three images taken from a 4DCT dataset, which illustrate the change of the tumor location as the patient breaths from full exhalation (0EX) to full inhalation (100IN).

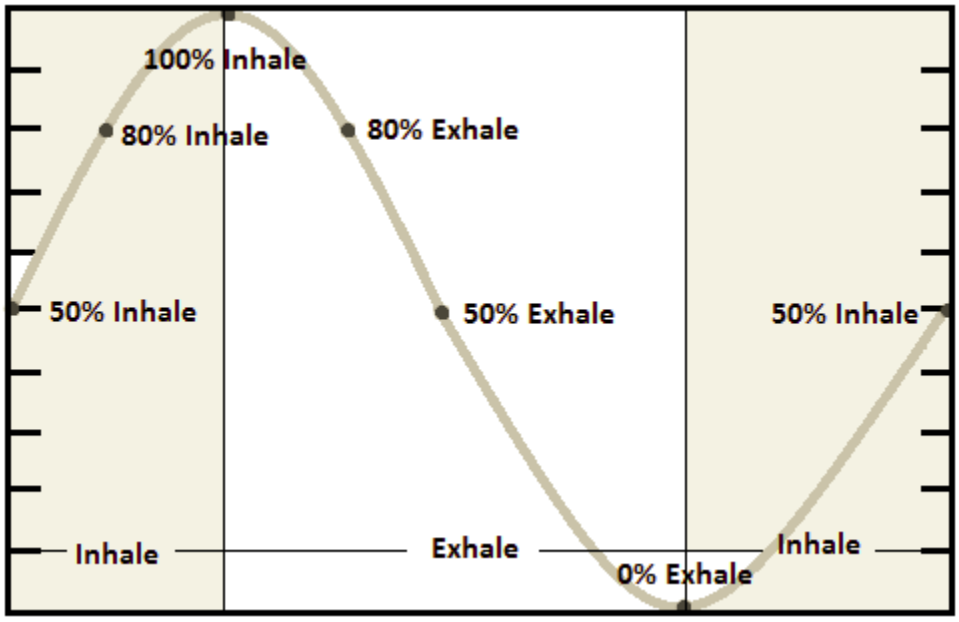

Figure 1. Respiratory trace cycle. Phases are identified based on the percentage of full inhalation or full exhalation that the lung has reached. The 50% inhale (50IN), 80% inhale (80IN), 100% inhale (100IN), 80% exhale (80EX), 50% exhale (50EX), and 0% exhale (0EX) respiratory phases have been marked.

www.manaraa.com

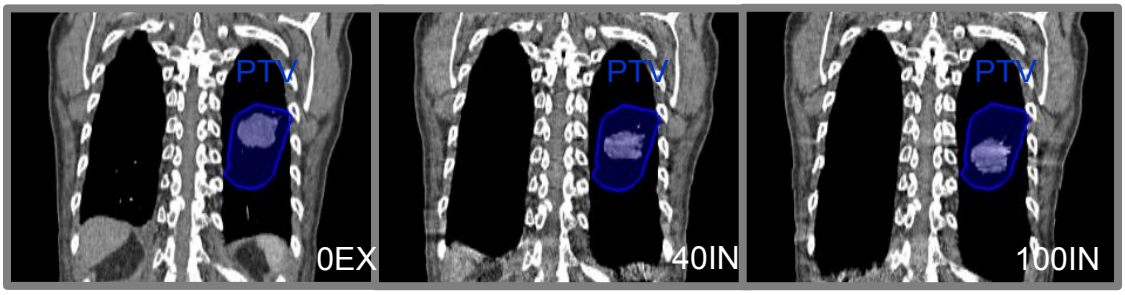

Figure 2. Sample images taken from a 4DCT dataset. From left to right, the images represent the 0EX phase in which the patient is at full exhalation, the 40IN phase, in which the patient is at 40% of full inhalation, and the 100IN phase in which the patient has reached full inhalation.

We examined two practices in which 4DCT is used in radiotherapy treatment planning for lung cancer. In Chapter 2, we compare 3-Dimensional (3D) dose calculation using a conventional breath-hold CT to 4-Dimensional (4D) dose calculation using 4DCT. Furthermore, we investigate the dosimetric uncertainty in 4D dose calculation using three different temporal probability distributions: uniform distribution, sinusoidal distribution, and patient-specific distribution derived from the patient's respiratory trace. Chapter 3 studies the dosimetric and temporal effects of respiratory gated radiation therapy. During gated treatment, radiation is only delivered when the patient is within a specific window of the respiratory cycle, thereby reducing the size of the target volume and increasing the amount of lung tissue spared. However, a tradeoff exists between the size of the gating window and the length of time required for delivery. Using 4DCT, we evaluated the dosimetric effects of four different gating windows, and estimated the corresponding treatment delivery times for normal (500MU/min) and high (1500MU/min) dose rates.

المنارة للاستشارات
www.manaraa.com

1.1 Background

Lung cancer remains the leading cause of cancer deaths in both men and women, expecting to account for an estimated 159,260 fatalities in the year 2014 [1]. As with most cancers, early detection and treatment are critical for an optimal outcome. In lung cancer treatment, several factors are considered, including the type of cancer (small cell (14% of patients) vs. non-small cell (84% of patients)), stage of disease, and histology of the cancer cells [1]. Treatments may include surgery, radiation therapy, chemotherapy, and other targeted therapies, and may also be combined to further improve results. The focus of our studies is upon patients who have undergone forms of radiation therapy. Radiation therapy involves the use of high-energy x-ray beams delivered to the cancer site in an effort to kill or stop the growth of tumorous cells. Typically, treatments are delivered in multiple fractions over a specified period of time. Radiation therapy may be used as the main course of treatment when a patient is not healthy enough for surgery or the cancer has spread too extensively for surgery to be a viable option [3]. In other cases, radiation therapy may be used as a combination treatment before surgery to shrink the tumor, or after surgery to kill any remaining tumor cells near the tumor bed. Radiation therapy may come from an external radiation source, known as external-beam radiation, or from an internal or implanted radiation source, known as brachytherapy. For these studies, we focus on external-beam radiation therapies.

1.1.1 Intensity-Modulated Radiation Therapy

Historically, 3D Conformal Radiation Therapy has been the standard radiotherapy for treating lung cancers. Using this technique, four to six radiation beams are planned with each beam collimated to the target volume to provide a uniform intensity

www.manaraa.com

distribution [5]. Intensity-Modulated Radiation Therapy (IMRT) was developed in an effort to further conform the dose distribution to the target volume, in doing so, sparing normal structures and allowing for an increased dose to be targeted at the cancer. IMRT allows for the intensity distribution within each beam to be optimized to give a desired dose distribution [5, 21]. Using a multileaf collimator, the treatment area is divided into multiple fields (i.e. beams), with each field divided into subfields (control points). Treatment delivery can either be static: subfields are treated using a uniform intensity and are superimposed to create the desired dose distribution, the beam is turned off while the leaves are positioned to create the next subfield, called the "step-and-shoot" or "stop-and-shoot" method, or dynamic: the beam is kept on while the leaves sweep with differing velocities to create the desired dose distribution, called the "sliding window," "leaf-chasing," "camera-shutter," or "sweeping variable gap" method [22]. Intensity-modulated arc therapy rotates the gantry while shaping the leaves, keeping the radiation beam on at all times. This method is similar to the "step-and-shoot" in that the subfield intensities are superimposed to give the desired distribution. Treatments typically require three to five arcs (more/less depending on the complexity of the treatment), with each arc designed to deliver one subfield at each gantry angle [22]. IMRT typically involves doses between 1-3Gy/fraction, delivered for 10-30 fractions [23].

1.1.2 Stereotactic Body Radiation Therapy

Stereotactic Body Radiation Therapy (SBRT), a treatment in which ultrahigh doses of radiation are delivered to the target, was initially used to treat lung cancers in the late 1990s. This technique developed from Stereotactic Radiosurgery (SRS), which was originally designed for treating cancers within the head and was much later regulatory

www.manaraa.com

approved to treat other sites within the body [3]. The main distinction of SBRT is the ability to provide a large dose in a few fractions. Typical SBRT dose ranges from 6-30Gy/fraction, delivered for 1-5 fractions [23]. Similar to IMRT, SBRT has two main objectives: The first objective is to more effectively kill cancer cells and reduce the risk of recurrence. This is done by delivering ultrahigh doses of radiation precisely targeted at the tumor. The second is to minimize the collateral damage done to healthy lung structures. This is achieved through a rapid dose falloff gradient, reducing the dose received by surrounding tissues [3, 24]. Like IMRT, SBRT uses a multileaf collimator for intensity modulation. Confidence in the accuracy of the treatment is critical for SBRT because of the ultrahigh dose rates involved. Typically, SBRT is used to treat well-circumscribed tumors, no larger than 5-7cm in diameter [23].

1.1.3 Treatment Planning

The first step involved in radiation therapy treatment planning for lung cancer is imaging. The most common imaging modality used is conventional 3D computed tomography (CT). Typically, a breath-hold CT scan is taken at end-of-exhale in order to reduce motion artifacts. Some institutions may also require a 4DCT scan in order to assess the need for respiratory management [14, 15]. Additionally, patients may undergo a positron emission tomography (PET) scan to help identify active tumor sites. Once imaging has been acquired, the next step is to contour the target and normal structures. Through treatment planning software, the CT scan is used to first contour the tumor, creating a gross tumor volume (GTV), see Figure 3. This GTV is then expanded in size in order to account for internal movement such as breathing- termed the internal target volume (ITV). Next, additional margins are added to the ITV to compensate for

www.manaraa.com

uncertainties due to planning and patient setup. This is termed the planning target volume (PTV) [15].

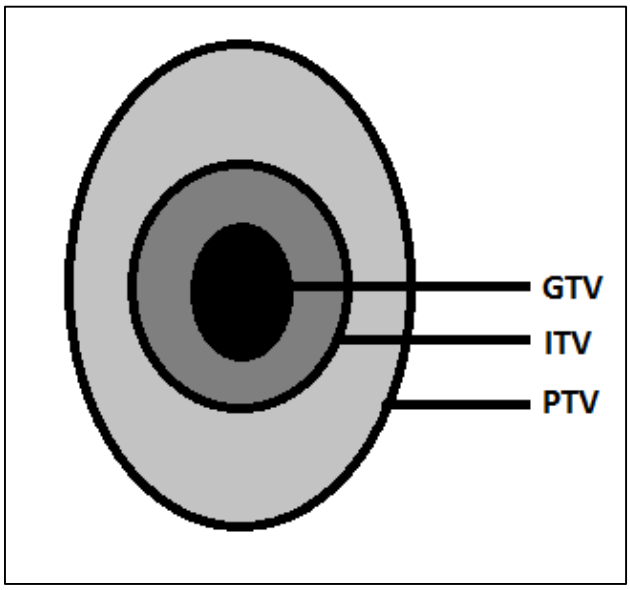

Figure 3. Delineation of target volumes for radiation therapy. The GTV is the gross tumor volume, ITV is the internal target volume, accounting for uncertainties in internal movement, and PTV is the planning target volume, accounting for uncertainties in planning setup.

Once all of the PTV and normal structures have been contoured, a set of dose objectives can be defined for each structural region. The treatment planning software can then be used to optimize a beam arrangement and calculate dose based on this set of objectives. In order to evaluate the 3D treatment plans in 2D, a histogram is used to compare radiation dose versus tissue volume for each structure- termed the dose-volume histogram or DVH. Other dosimetric evaluation criteria include the mean tumor dose (MTD), mean lung dose (MLD), and lung V20 (percent of the lung volume receiving more than 20 Gy).

www.manaraa.com

1.1.4 Monitoring Respiratory Motion

Respiration-induced tumor motion can yield large uncertainties in target delineation and localization. Unfortunately, it is not possible to generalize respiratory behavior for a particular patient prior to observation and treatment [6]. The American Association of Physicists in Medicine (Task Group 76) has recommended that respiratory management methods should be considered when the range of tumor motion for a given patient exceeds 5mm in any direction [6]. Various techniques have been presented in an effort to characterize and reduce the impact of respiratory motion during radiotherapy [25, 26]. These include respiratory gated techniques, breath-hold techniques, forced shallow breathing methods, and real-time tumor tracking methods [6]. Current commercial patient respiratory monitoring systems primarily use either an external respiratory signal or internal fiducial markers. Two widely used systems are the Anzai Respiratory Gating System (Anzai medical Co. Ltd, Tokyo, Japan) and the Varian Real-Time Position Management [RPM] System (Varian Medical Systems, Palo Alto, CA). The Anzai system uses a strain gauge pressure sensor fixed to the upper abdomen using an elastic belt to record changes in pressure applied to the sensor as the patient breathes. The RPM system positions a lightweight block containing two reflective markers on the upper abdomen and uses an infrared light and camera to capture the depth of motion. Though collecting these external respiratory signals is much less invasive than placing implanted markers, some uncertainty remains between the correlation of the internal tumor motion and the movement of the external surrogate [27]. Additionally, these external methods are limited to capturing motion in one dimension. However, placement and tracking of internal markers accompanies its own set of challenges, including a high

www.manaraa.com

risk of pneumothorax from insertion and additional radiation exposure from fluoroscopic imaging [27].

1.1.4 4D Dose Calculation using 4DCT

As described in the introduction, 4D dose calculation accounts for the position of the tumor at multiple phases of respiration and is therefore expected to provide a more realistic dose distribution than conventional 3D dose calculation. To calculate a 4D dose distribution using 4DCT, dose is firstly computed for each phase CT, then mapped to the breath-hold CT by deformable image registration. This essentially gives several 3D dose volumes, one for each respiratory phase, that must be summed together to create one 4D volume. Since studies have shown that patients do not spend an equal amount of time in each respiratory phase [8, 11, 12], ideally each dose should be weighted according to the fraction of time the patient spends at that particular respiratory amplitude (i.e. the temporal probability) [13]. We can obtain these temporal probabilities from the patient's respiratory trace, which can be collected through various methods as described in 1.1.4. However, in cases when the patient's respiratory trace is not readily available, it is unclear whether an approximated temporal probability distribution may be used.

www.manaraa.com

CHAPTER 2: FOUR-DIMENSIONAL DOSE CALCULATION

2.1 Literature Review

Several methods [15] have been proposed for 4D dose calculation, where respiratory motion was incorporated by either using patient-specific temporal probabilities from their respiratory traces [13, 15] or modelling the tumor's trajectory. Many studies approximated tumor motion as a sinusoidal respiratory model [28-30]: Lujan et al. [29], George et al. [28], and Bortfeld et al. [30] presented sinusoidal probability distribution functions (PDFs), which modeled the tumor's motion as being periodic, while asymmetric, accounting for increased time spent in the exhalation phase. These studies computed 4D dose by convolving the 3D static dose distribution with the PDF of the tumor's motion [15, 28-30]. Lax et al. [31] also used a similar convolution method to compare dose distributions for SBRT cases using four different probability distribution functions: linear, harmonic oscillator, patient data with fixed amplitude and frequency, and patient data with variances in amplitude and motion pattern. They found that the differences in dose distributions were relatively small among the four PDFs. However, this study was limited to phantom images.

More recent 4D dose calculation studies have employed 4DCT images: Rietzel et al. [14] and Guckenberger et al. [13] used deformable image registration to calculate delivered dose in the presence of respiratory motion. They assumed equal weighting between respiratory phases because the binned CT data were uniformly distributed across a respiratory cycle. Similarly, Guerrero et al. [32] also used equal fractional weighting when combining doses for 4D mapping in their phantom thoracic radiotherapy study, and Flampouri et al. [20] used similar 4D calculation methods to study delivered dose in

www.manaraa.com

IMRT patients. To the best of our knowledge, no 4D dose calculation studies utilizing 4DCT have yet been conducted to explicitly evaluate the dosimetric effects of using different temporal probabilities.

We have previously investigated the dosimetric difference between 3D and 4D dose calculation using the same image acquisition and dose calculation methods as described in 2.2.1-2.2.3 [33]. Figure 4 shows the results of this study. Compared to 3D dose calculation, lung V20, mean lung dose (MLD), and mean tumor dose (MTD) using 4D- dose calculation on average differed by 0.7% ± 2.1%, 4.8% ± 8.4% (0.4 Gy ± 0.9 Gy), and 1.2% ± 1.4%(0.7 Gy ± 0.9 Gy), respectively. These findings suggested that conventional 3D dose calculation may overestimate lung V20, MLD, and MTD, though, the absolute difference between 3D and 4D dose calculation in lung tumors may not be clinically significant.

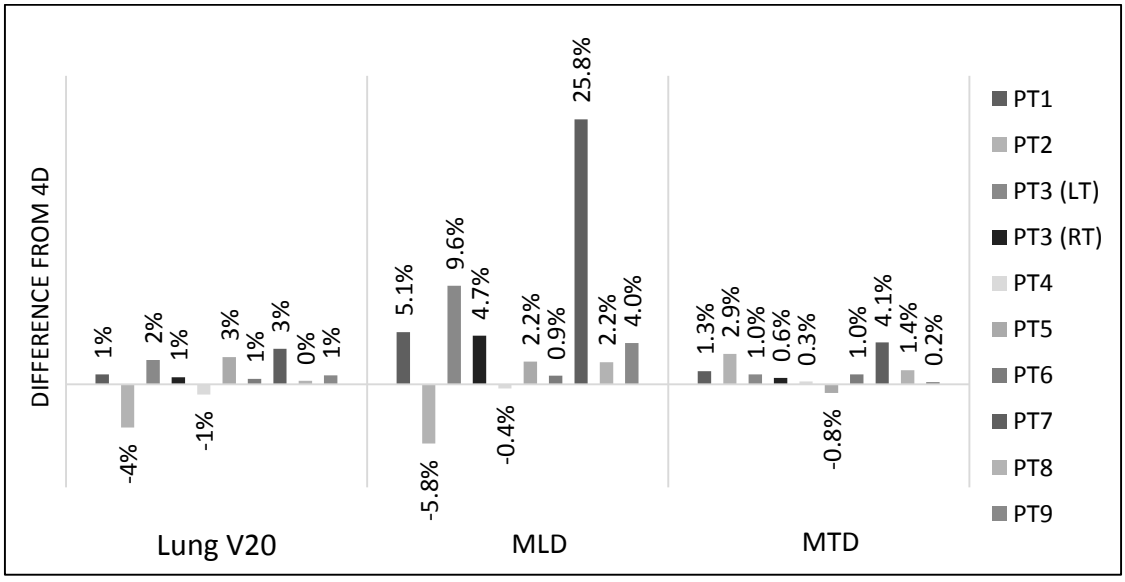

Figure 4. Dosimetric difference between 3D and 4D dose calculation. As compared to 4D dose calculation, 3D calculation appears to overestimate lung V20, MLD, and MTD.

www.manaraa.com

2.2 Study Objective

The objective of this study was to investigate the dosimetric uncertainty in 4D dose calculation using three different temporal probability distributions: uniform distribution, sinusoidal distribution, and patient-specific distribution derived from the patient's respiratory trace.

2.3 Methods

After institutional review board approval (#200905703, University of Iowa), treatment plans for nine lung cancer patients were retrospectively evaluated. A summary of patient characteristics is listed in Table 1, where maximum tumor motion varied from 3 to 23 mm. Among the nine patients, five of them were treated using stereotactic body radiation therapy, while the remaining four were treated using intensity-modulated radiation therapy. Gated radiation therapy was used in four patients.

Table 1. Summary of patient characteristics.

Patient	Lung Volume (cm^3)	PTV Volume (cm^3)	Tumor Motion (mm)	Treatment	Gated Therapy
P1	816	14	6	SBRT	Yes
P2	2,103	236	15	IMRT	Yes
P3(LT)	1,872	160	23	SBRT	Yes
P3(RT)	2,383	17	3	SBRT	No
P4	791	97	10	IMRT	No
P5	733	578	3	IMRT	No
P6	1,859	110	8	SBRT	No
P7	1,502	33	10	SBRT	No
P8	1,018	115	12	IMRT	Yes
P9	1,695	141	10	SBRT	No

www.manaraa.com

2.3.1 Image Acquisition

Patient CT images were acquired using the Siemens Biograph™ PET-CT scanner (Siemens Medical System, Knoxville, TN). For each patient, a breath-hold CT scan at the end of exhale was first taken, followed by a 4DCT scan, where the patient's respiratory trace was recorded using a strain gauge pressure sensing system (Anzai medical Co. Ltd, Tokyo, Japan). For each 4DCT scan, ten phase CT images were reconstructed, representing ten different respiratory phases.

2.3.2 3D Dose Calculation

The Pinnacle^3 treatment planning system (Philips Radiation Oncology Systems, Milpitas, CA) was used for treatment planning. For 3D calculation, the treatment plan was based on the exhale breath-hold CT scan. Tumor motions from the 4DCT images were used to create the internal target volume (ITV). Planning target volume (PTV) was delineated by adding 5 mm margins to the ITV in the anterior-posterior, medial-lateral, and cranio-caudal directions.

2.3.3 4D Dose Calculation

For each patient, three 4D dose volumes were computed, corresponding to three temporal probability distributions. A summary of the workflow is shown in Figure 5. First, the corresponding dose for each of the 10 binned phase CTs was calculated using the same planning parameters as those used in 3D dose calculation. Next, the 10 binned CTs and their corresponding doses were imported into the VelocityAI software (Velocity Medical Systems, Atlanta, GA). Deformable image registration was then used to compute the deformation map between each binned CT and the breath-hold CT. This deformation map was applied to the corresponding dose on each binned CT to generate the deformed

www.manaraa.com

phase dose. Finally, a MATLAB (MathWorks, Natick, MA) algorithm was used to generate a four-dimensional dose volume by summing the 10 deformed phase doses with respect to each of three temporal probability distributions: 1) uniform distribution, 2) sinusoidal distribution, and 3) patient-specific distribution derived from the patient's respiratory trace. The 4D dose is calculated by

$$Dose_{4D} = \sum_i P_i \times DeformedPhaseDose_i \quad (1)$$

where i represents the respiratory phase, P_i is the temporal probability for phase *i*, and $DeformedPhaseDose_i$ is the deformed dose for phase i.

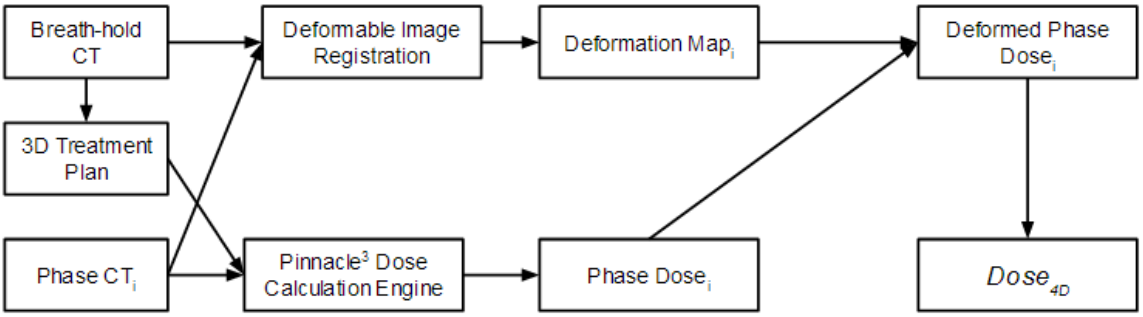

Figure 5. Workflow for 4D dose calculation. Four-dimensional (4D) CT and deformable image registration were used to compute 4D radiation dose incorporating the patient's respiratory motion. First, the dose for each of 10 phase CTs was computed using the same planning parameters as those used in the three-dimensional (3D) treatment plan. Next, deformable image registration was used to deform the dose of each phase CT to the breath-hold CT using the deformation map between the phase CT and the breath-hold CT. Finally, a 4D dose volume was computed by summing the 10 deformed doses using their corresponding temporal probabilities.

2.2.4 Dosimetric Evaluation

In this study, 4D dose calculated using patient-specific temporal probabilities was used as the ground truth and compared against 4D doses calculated using uniform and sinusoidal temporal probability distributions.

www.manaraa.com

2.3.4.1 Gamma Analysis

3D gamma analysis [34, 35] was used to evaluate the 4D dose volumes. The basis for calculating gamma value (γ) is given in Equation 2, where r is the reference dose distribution (e.g. patient-derived distribution), e is the evaluated dose distribution (e.g. sinusoidal or uniform distribution), r is the spatial distance, D is dose, ΔD is the dose difference criterion, and Δd is the distance to agreement criterion. Gamma passing rate was defined as the percentage of the volume whose gamma value is equal to or less than 1. In this study, dose difference (ΔD) and distance to agreement (Δd) criteria were 3% and 3mm, respectively. An open source MATLAB (MathWorks, Natick, MA) algorithm (Threaded 3D Gamma, University of Western Ontario, London, ON) was used to calculate a 3D gamma volume, which was then imported into the VelocityAI software (Velocity Medical Systems, Atlanta, GA) for analysis. 3D gamma analysis was conducted twice for each patient, first comparing the ground truth calculation to dose calculation using a uniform temporal probability distribution and again comparing the ground truth calculation to dose calculation using a sinusoidal temporal probability distribution. In each case, the gamma passing rate was computed for two common structures: the lung and the PTV.

$$\gamma(r_e) = \min\{\Gamma(r_r, r_e)\} \forall \{r_e\} \qquad (2)$$

where

$$\Gamma(r_r, r_e) = \sqrt{\frac{(r_e - r_r)^2}{\Delta d^2} + \frac{(D_e(r_e) - D_r(r_r))^2}{\Delta D^2}}$$

2.2.4.2 Mean Lung Dose, Mean Tumor Dose, and Lung V20

As a measure of clinical impact, mean lung dose (MLD), mean tumor dose

www.manaraa.com

(MTD), and lung V20 (percentage of the lung volume receiving at least a 20Gy dose) were evaluated for each dose volume. To do so, the VelocityAI software (Velocity Medical Systems, Atlanta, GA) was used to generate and analyze the dose-volume histogram. Percentage and absolute differences in measures were computed between the ground truth and the approximated dose volumes.

2.4 Results

2.4.1 Gamma Analysis

Figure 6 shows the gamma passing rates. 4D Dose computed using uniform and sinusoidal temporal probability distributions both passed the 95% gamma acceptance criteria across all patients for the lung and the PTV. Gamma passing rates for the lung were greater than 99% for all calculations with the exception of P4, which had a passing rate greater than 97% when using uniform or sinusoidal distributions. Gamma passing rates were also greater than 99% for the PTV with the exception of the uniformly-distributed dose volume of P8, which had a passing rate greater than 98%.

www.manaraa.com

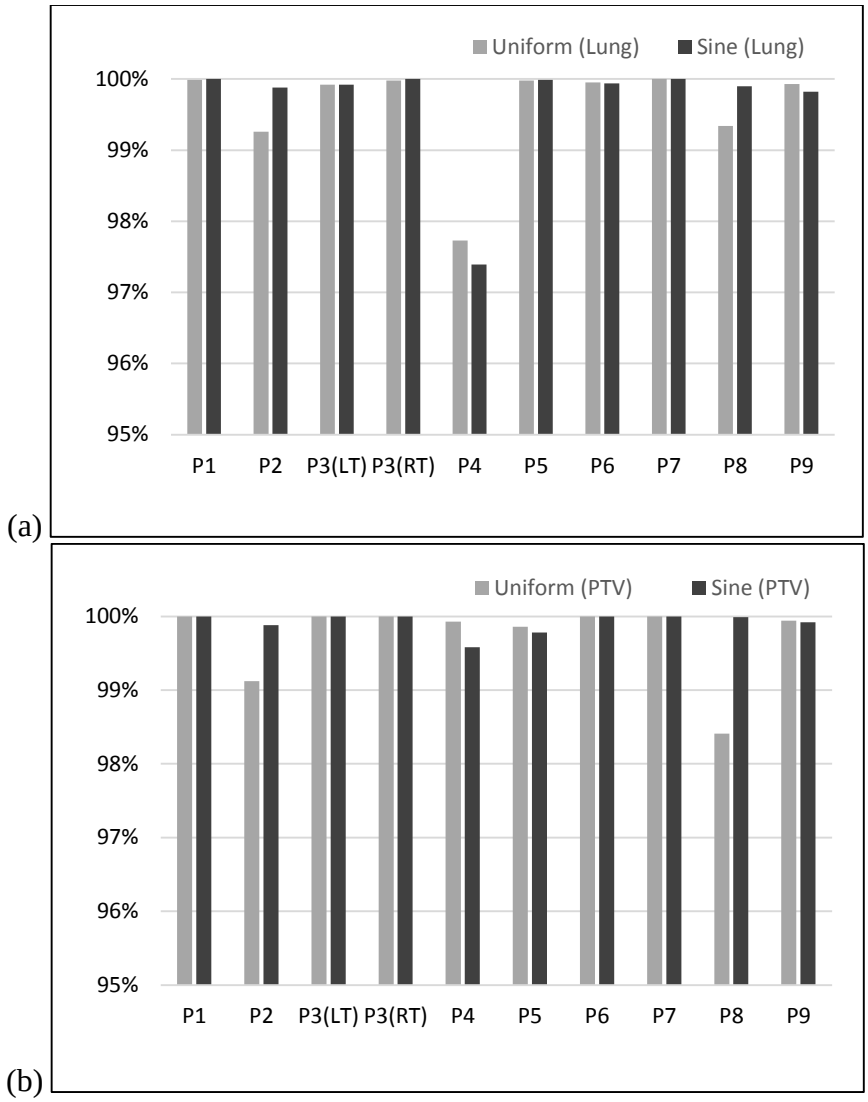

Figure 6. Gamma passing rate using 3% dose difference and 3mm distance to agreement criteria. For each patient, dose volumes computed using uniform and sinusoidal temporal probability distributions were evaluated against dose volumes using the patient respiratory trace distribution. (a) Gamma passing rate for lung; (b) Gamma passing rate for PTV.

2.4.2 Mean Tumor Dose

As shown in Figure 7, when compared with calculations using patient-specific temporal probabilities, those using uniform distribution and sinusoidal distribution showed a percentage difference on average of -0.1±0.6% and -0.2±0.4% in MTD,

www.manaraa.com

respectively. For all patients, the percentage difference in MTD was less than 1% when using uniform or sinusoidal distributions and absolute difference in MTD was less than 1Gy.

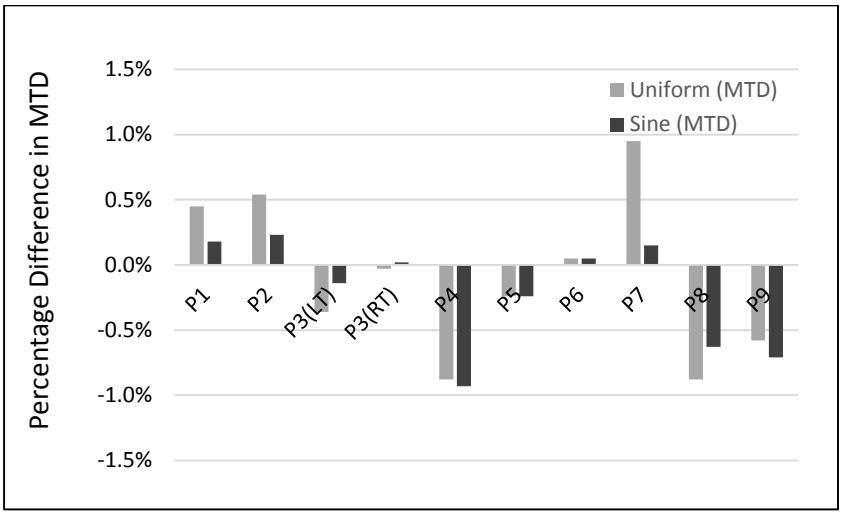

Figure 7. Percentage difference in mean tumor dose for uniform and sinusoidal temporal probability distributions as compared to patient-specific distributions.

2.4.3 Mean Lung Dose

As shown in Figure 8, on average, percentage difference in MLD was found to be -0.2±2.0% and -0.2±1.3% when using uniform and sinusoidal dose distributions, respectively. Some patients appeared to exhibit a greater percentage difference in MLD, however, the absolute difference in the calculated measurements for all patients was very small. Patient P1 showed the greatest percentage difference in MLD, 4.4% and 2.7%, respectively when using uniform and sinusoidal distributions. However, the absolute difference for this patient was only 0.2Gy and 0.1Gy, respectively for uniform and sinusoidal distributions.

www.manaraa.com

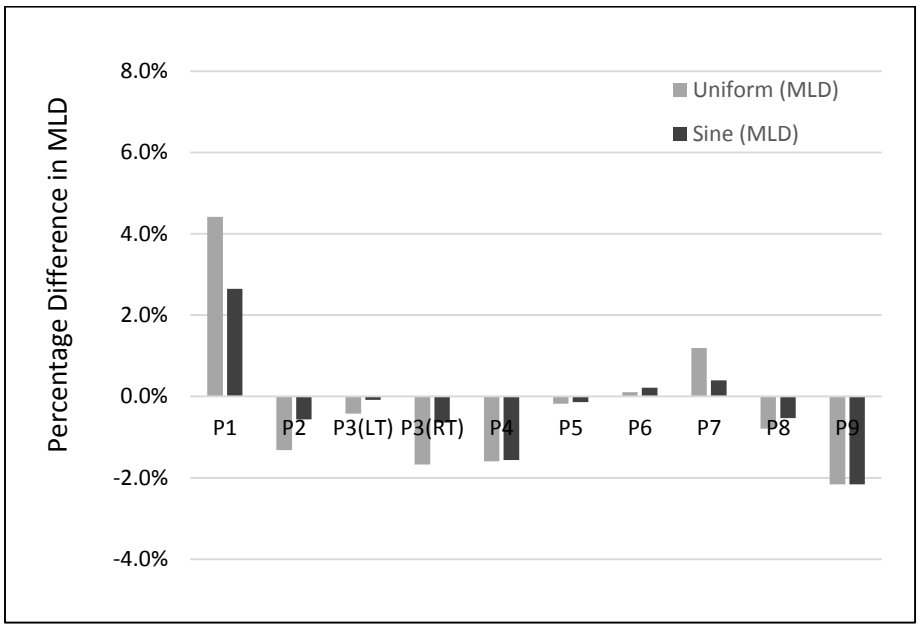

Figure 8. Percentage difference in mean lung dose for uniform and sinusoidal temporal probability distributions as compared to patient-specific distributions.

2.4.4 Lung V20

Figure 9 shows the percentage difference in patient lung V20. On average, lung V20 was 0.9±2.8% and -0.7±1.8%, respectively when using uniform and sinusoidal distributions. Patient P1 again had the greatest percentage difference, 7.1% and 4.0% difference in lung V20, respectively for uniform and sinusoidal distributions. Again, the absolute difference in value for this patient is very small, 0.5% and 0.28%, respectively for uniform and sinusoidal distributions.

www.manaraa.com

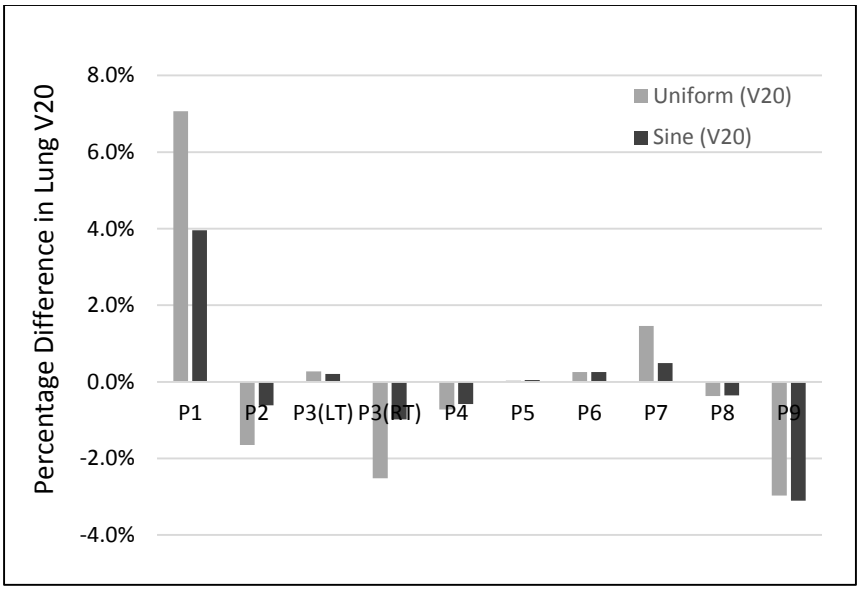

Figure 9. Percentage difference in lung V20 for uniform and sinusoidal temporal probability distributions as compared to patient-specific distributions.

2.5 Discussion

Average gamma passing rate was greater than 99% for 4D dose calculations computed using both uniform and sinusoidal temporal probability distributions, exceeding the 95% acceptance criteria. This suggests that 4D dose calculated using uniform or sinusoidal temporal probabilities are clinically comparable to the ground truth. Differences between 4D dose using uniform versus sinusoidal temporal probabilities were nominal. Compared with the uniform temporal probability distributions, sinusoidal distributions resulted in an equal or slightly better gamma passing rate in six out of nine patients, however, the magnitude of these differences was less than one percentage. Figure 10 shows a plot of the PTV gamma passing rates as compared to tumor motion. Standard deviation between gamma passing rates was less than 1%. Because the majority of gamma passing rates were very similar, no definitive correlations could be drawn between the tumor motion and the gamma passing rate from these nine subjects.

www.manaraa.com

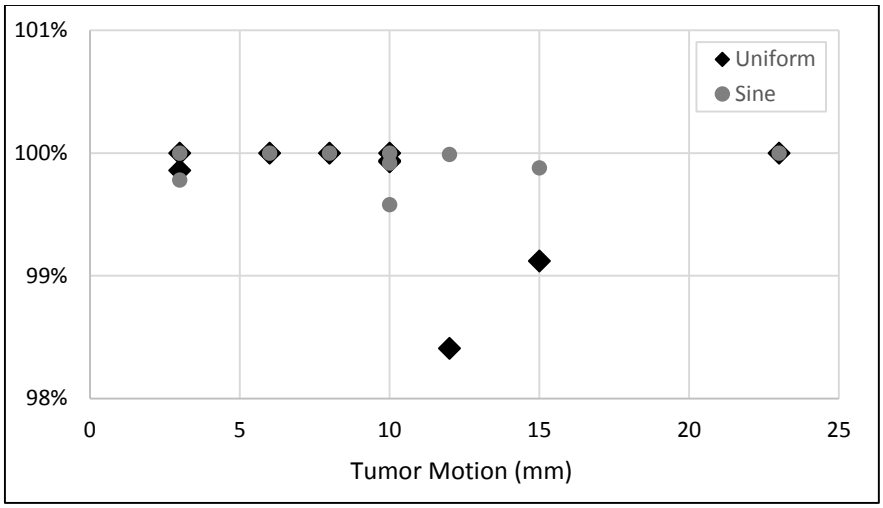

Figure 10: The gamma passing rates for the PTV with respect to the magnitude of the tumor's motion. Because the majority of gamma passing rates were very similar, no definitive correlations could be drawn between the tumor motion and the gamma passing rate.

When comparing to the ground truth, the absolute dosimetric differences of mean tumor dose and mean lung dose of the uniform and sinusoidal temporal probability dose volumes were within 1Gy for all subjects, indicating that dose can be clinically approximated for the lung and the PTV using both uniform and sinusoidal temporal probability distributions. As shown in Figures 7-9, the overall difference for the sinusoidal temporal probability distribution was smaller than that for the uniform distribution. This difference may be due to patients spending more time in the end-exhale (0EX) phase (Figure 11), which could be better represented by the sinusoidal distribution. However, the difference between the uniform distribution and the sinusoidal distribution was small. We attempted to compare the dosimetric differences of the dose volumes against the magnitude of the tumor motion and the size of the PTV, however, because differences between the uniform, sinusoidal, and ground truth dose volumes were very small, we were unable to identify any correlations.

www.manaraa.com

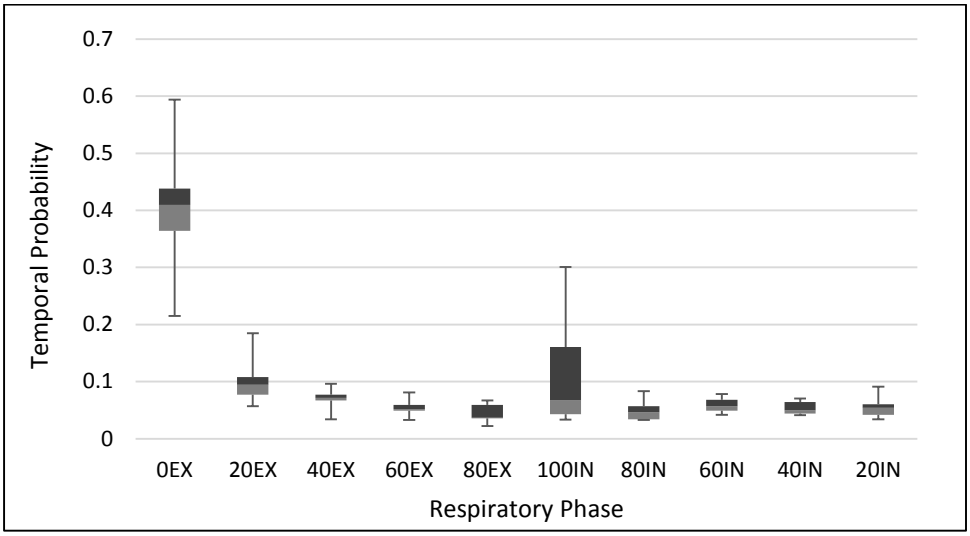

Figure 11. Free breathing patient temporal probability distributions where EX and IN refer to exhalation and inhalation phases, respectively, and preceding phase numbers refer to the percentage of full inhalation. Patients spent the majority of their time in the end-exhale (0EX) phase - on average of 45%±12%.

Lung V20 is often used clinically as a dose constraint for lung complications [17]. The absolute difference in lung V20 for the uniform and sinusoidal temporal probability dose volumes was within 1% for all calculations when comparing to the ground truth volume. This is consistent with the previously stated MTD and MLD results and again suggests that the two approximated dose volumes and the patient-specific dose volume are clinically very similar.

Ideally, to compute 4D dose, the temporal probability should be derived from the patient-specific respiratory trace. However, respiratory motion can vary from day to day, especially in patients with poor pulmonary function [6, 9], therefore the range of motion obtained at the time of the CT scan may vary from the range of motion observed during the time of treatment delivery. Furthermore, some institutions may find obtaining the

www.manaraa.com

respiratory trace an added inconvenience. Our results may suggest that 4D dose volumes can be approximated in the absence of respiratory trace data.

In the future, it would be interesting to investigate whether the accuracy of the approximated dose volume is in any way correlated to the tumor motion or size of the PTV. With the current data, differences across the uniform, sinusoidal, and ground truth dose volumes were not sufficient to be able to draw these conclusions. By using more selective gamma tolerance criteria, differences across the three 4D dose volumes may become more apparent.

www.manaraa.com

CHAPTER 3: GATED RADIATION THERAPY

3.1 Literature Review

Respiratory gated radiation therapy (RGRT) involves monitoring the respiratory signal and only delivering radiation when the patient is within a specific window of the respiratory cycle, thereby reducing the size of the target volume and increasing the amount of normal tissue spared. Several recent studies using 4DCT have shown that the use of patient-specific treatment margins and respiratory gating, rather than standard population-based treatment margins can reduce normal tissue toxicity [19, 25, 26, 36, 37]. However, some have pointed out that the additional dosimetric benefits from respiratory gating are modest and do not justify the challenges of RGRT, including the increased time for treatment delivery and, consequently, the increased potential for uncertainty introduced from patient movement [27, 36]. Currently, no established guidelines concerning the use of respiratory gating have been defined [25, 27].

Treatment delivery during gated therapy is not continuous, and as a result, total time of treatment is prolonged due to the decreased duty cycle (i.e. percentage of time during which the beam is active). Various gating methods have been suggested, though a limited number of publications were found to report on treatment times for gated radiation therapy [38-40] . One common method for reducing gated treatment times involves the use of breath-hold during treatment delivery. Berson *et al.* [38] compared gated therapy using breath-hold coaching versus free breathing without coaching and found that treatment times decreased from 4.0 min/100 MU to 2.0 min/100MU. Similarly, Linthout *et al.* [39] found that they were able to reduce gated delivery time through voluntary breath-hold with the assistance of audio-visual feedback. Average

www.manaraa.com

gated delivery time in their study decreased from 1.7 min/100 MU to 1.4 min/100 MU with the introduction of visual assistance and further decreased to 0.9 min/100 MU with additional audio assistance. Increasing the delivery dose rate has also been suggested for reducing gated treatment times. In the previously mentioned study by Linthout *et al.* [39], preliminary results showed that increasing the dose rate from 480 to 800 MU/min further decreased treatment delivery time from 0.9 min/100 MU to 0.4 min/100MU. Likewise, Willoughby *et al.* [40] found that increasing dose rate from 480 to 800 MU/min reduced gated treatment times by 40% when using 20% and 40% gating windows, while maintaining an output consistency within 0.5%.

3.2 Study Objective

The objective of this study was to measure the dosimetric and temporal effects of respiratory gated radiation therapy. Although gated treatment has been shown to reduce normal lung toxicity, increased risks due to prolonged treatment times are often cited as a concern. We evaluated the dosimetric impacts of four gating windows and estimated the corresponding treatment delivery times using normal (500MU/min) and high (1500MU/min) dose rates.

3.3 Methods

Following institutional review board approval (#200905703, University of Iowa), five lung cancer patients treated at our institution were included in this retrospective study. All of the patients had undergone 4DCT scans. A summary of patient characteristics is listed in Table 2. Among the patients, maximum tumor motion varied from 6 to 12 mm. Two patients were treated with respiratory gating using an 80EX-80IN gating window (Table 3), while three patients were treated without respiratory gating. Of

www.manaraa.com

the patients, one was treated with intensity-modulated radiation therapy, while the remaining four were treated using stereotactic body radiation therapy.

Table 2. Summary of patient characteristics.

Patient	Lung Volume (cm^3)	PTV Volume (cm^3)	Max Tumor Motion (mm)	Prescription Dose (Gy)	Treatment	Gated Therapy
P1	816	14	6	50	SBRT	Yes
P6	1,859	110	8	40	SBRT	No
P7	1,502	33	10	54	SBRT	No
P8	1,018	115	12	61.2	IMRT	Yes
P9	1,695	141	10	40	SBRT	No

3.3.1 Image Acquisition

Patient CT images were acquired using the Siemens Biograph™ PET-CT scanner (Siemens Medical System, Knoxville, TN). For each patient, a breath-hold CT scan at the end of exhale was first taken, followed by a free breathing 4DCT scan, during which the patient's respiratory motion was recorded using a commercially available strain gauge pressure sensing system (Anzai medical Co. Ltd, Tokyo, Japan) fixed to the upper abdominal region using an elastic belt. Retrospective sorting of the 4DCT projections was performed using the CT console. Each reconstructed CT image corresponded to one of 10 respiratory amplitudes, representing ten different respiratory phases: 0EX, 20EX, 40EX, 60EX, 80EX, 100IN, 80IN, 60IN, 40IN, and 20IN, see figure 1.

3.3.2 Deriving Target Volumes

For each patient, the breath-hold CT scan was used to generate the original gross tumor volume (GTV) used at the time of treatment. Contouring was performed using the

www.manaraa.com

Pinnacle^3 treatment planning system (Philips Radiation Oncology Systems, Milpitas, CA). This GTV was automatically copied to each 4DCT dataset using deformable image registration software (Velocity Medical Systems, Atlanta, GA). GTVs for each phase CT were verified and sparsely edited as needed to ensure they conformed to the corresponding 4DCT image. Four internal target volumes (ITVs), corresponding to four gating windows (Table 3), were then created by summing the GTVs for each phase included within the gating window.

Table 3. Gating Windows.

Gating Window	Included Phases
20EX-20IN	20EX, 0EX, 20IN
40EX-40IN	40EX, 20EX, 0EX, 20IN, 40IN
60EX-60IN	60EX, 40EX, 20EX, 0EX, 20IN, 40IN, 60IN
80EX-80IN	80EX, 60EX, 40EX, 20EX, 0EX, 20IN, 40IN, 60IN, 80IN

Treatment planning was performed using the Pinnacle^3 treatment planning system (Philips Radiation Oncology Systems, Milpitas, CA). Planning target volumes (PTVs) were derived from ITVs by adding additional 5mm margins, accounting for uncertainty in patient setup. The four PTVs were then used to generate four individual treatment plans satisfying the same planning criteria as the original treatment plan.

3.3.3 Dosimetric Evaluation

Mean tumor dose (MTD), mean lung dose (MLD), and lung V20 (percentage of the lung volume receiving at least a 20Gy dose) were used for dosimetric evaluation. The Pinnacle^3 treatment planning system (Philips Radiation Oncology Systems, Milpitas, CA) was used to generate and analyze the dose-volume histogram. Percentage and absolute

www.manaraa.com

differences were computed between the gated and original treatment plans.

3.3.4 Calculation of Treatment Time

A MATLAB (MathWorks, Natick, MA) algorithm was developed to compute the treatment time for each plan, including time for gantry rotation, time for collimator leaves and jaws motion, time to deliver dose, and time for communication overhead. For gated treatment plans, time to deliver dose was scaled relative to the time spent within the gating window based on the patient's respiratory trace. Treatment times were first compared using dose rates of 500 MU/min for both gated and non-gated treatment plans, then compared again using an increased dose rate of 1500 MU/min for gated plans.

3.3.4.1 Treatment Time Algorithm

The MATLAB (MathWorks, Natick, MA) algorithm created was designed to compute the treatment delivery time by utilizing the treatment information exported from the Pinnacle[3] treatment planning system (Philips Radiation Oncology Systems, Milpitas, CA), (see Figure 12). Equation 3 describes the calculation for total treatment time (t_{total}), where *beam* is the total number of beams, $t_{overhead}$ is the time of communication overhead, t_{gantry} is the gantry rotation time, *CP* is the total number of control points, t_{mech} is the mechanical time for the collimator leaves and jaws, and t_{dose} is the time to deliver dose.

$$t_{total} = \sum_{k=1}^{beam} \left\{ t_{overhead_k} + t_{gantry_k} + \sum_{i=1}^{CP} t_{mech_i} + t_{dose_i} \right\} \quad (3)$$

Time of communication overhead ($t_{overhead}$) was defined as 3 seconds for each beam based on observation. This constant was included to account for machine communication time. Gantry rotation time (t_{gantry}), see Equation 4, was computed by calculating the difference between the current (θ_i) and previous (θ_{i-1}) beam angle (0˚ at start) and assuming a gantry rotation speed (s_{gantry}) of 3˚/sec based on observation of the gantry rotation.

www.manaraa.com

$$t_{gantry} = \frac{(\theta_i - \theta_{i-1})}{s_{gantry}} \quad (4)$$

Mechanical time (t_{mech}), calculated by Equation 5, accounts for the time to move the jaws and collimator leaves for each control point. First, an optimal sequence for the control points, that which gave the fastest time, was determined by finding the sequence requiring the least movement between control points. Next, for each control point, the distance moved by each leaf (*y)* and jaw (*j*) (based on current (*i*) and previous (*i-1*) position) was computed and divided by constants s_{leaf} and s_{jaw}, respectively for the leaves and jaws. For each control point, the maximum amount of time taken to move all leaves and jaws was defined as the mechanical time. In order to determine s_{leaf} and s_{jaw}, the treatment time algorithm was run for each patient using varying leaf and jaw speed combinations ranging from 0.1 up to 4.0cm/s. We chose 2.0cm/s for s_{leaf} and 1.0cm/s s_{jaw} because this combination provided a close estimate of the actual treatment time, and observation of the leaf and jaw movement of the linear accelerator was noted to be around this range, with jaws observed to be moving at approximately half of the speed of the leaves.

$$t_{mech} = Max\left\{\left(\frac{(y_i - y_{i-1})}{s_{leaf}}\right)\forall\{y\}, \left(\frac{(j_i - j_{i-1})}{s_{jaw}}\right)\forall\{j\}\right\} \quad (5)$$

Time to deliver dose (t_{dose}) was also calculated for each control point of the beam. Equation 6 defines the equation used for calculation. Number of monitor units for each control point (MU_{CP}) was first calculated by multiplying the total prescribed monitor units (MU_{total}) by the beam weighting (w_{beam}) and the control point weighting (w_{cp}). Time to deliver dose was then calculated by dividing MU_{CP} by the dose rate (*DR*) and Gating factor (*GF*). Gating factor was derived from the patient's respiratory trace and defined as

www.manaraa.com

the fraction of the respiratory signal contained within the gating window ($Resp_{GW}$) versus the total respiratory signal ($Resp_{total}$).

$$t_{dose} = \frac{MU_{CP}}{DR*GF} \quad (6),$$

where $MU_{CP} = MU_{total} * w_{beam} * w_{CP}$ and $GF = \frac{Resp_{GW}}{Resp_{total}}$

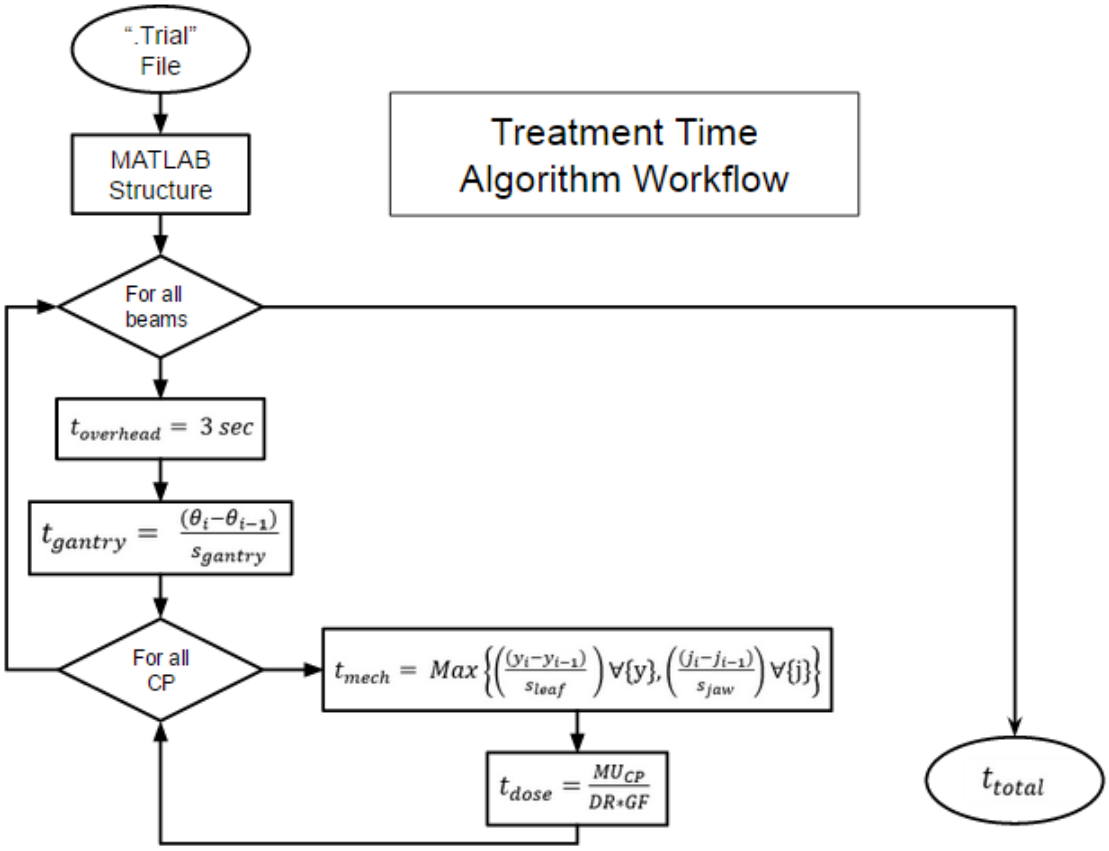

Figure 12. Workflow for treatment time calculation. The MATLAB (MathWorks, Natick, MA) inputs a ".Trial" file exported from the Pinnacle[3] treatment planning system (Philips Radiation Oncology Systems, Milpitas, CA), and outputs an estimate for treatment delivery time (t_{total}). Time for gantry rotation (t_{gantry}), time to position collimator leaves and jaws (t_{mech}), and time to deliver dose (t_{dose}) were considered, along with time of communication overhead ($t_{overhead}$).

www.manaraa.com

3.3.4.1 Validation of Treatment Time Algorithm

To validate the treatment time algorithm, actual treatment times for the five patients were obtained from the treatment record and verify system, MOZAIQ (Elekta, Stockholm, Sweden), and compared against computed treatment times using the patient's prescribed dose rate and gating window. Because patients received multiple fractions and visit times could vary depending on the consistency of breathing, the actual treatment time was defined as the average treatment time across visits. Any obvious outliers were excluded during calculation of the average treatment time.

3.3.5 Evaluation of Results

Patient results have been divided into two groups: 1) Patients treated using a non-gated treatment plan and 2) Patients treated using an 80EX-80IN gating window. In the first group, the evaluated 20EX-20IN to 80EX-80IN treatment plans are compared against the original non-gated plan. In the second group, the evaluated 20EX-20IN to 60EX-60IN treatment plans are compared against the original 80EX-80IN gated plan.

3.4Results

3.4.1 Dosimetric Evaluation

3.4.1.1 Non-gated Patients

Table 4 summarizes the percentage differences between the originally non-gated plans and their corresponding gated plans. The average reduction in PTV volume was -26.9±4.4%, -21.8±4.2%, -15.4±2.6%, and -9.4±6.0%, respectively for the 20EX-20IN to 80EX-80IN gated plans as compared to the non-gated plan (Figure 13). PTV coverage for all gated plans was kept within 1% of the original PTV coverage, and differences in MTD were calculated to be less than 1Gy across plans for all patients (Figure 14). As shown in

www.manaraa.com

Figures 15 and 16, MLD and Lung V20 were found to decrease as we reduced the gating window. On average, relative percentage differences in MLD and Lung V20 were reduced by -16.1±1.0% and -20.0±2.3%, -12.5±1.0% and -15.6±2.3%, -8.7±3.5% and -11.1±4.2%, -6.0±4.7% and -7.2±5.7%, respectively for the 20EX-20IN to 80EX-80IN gated plans as compared to the non-gated plan.

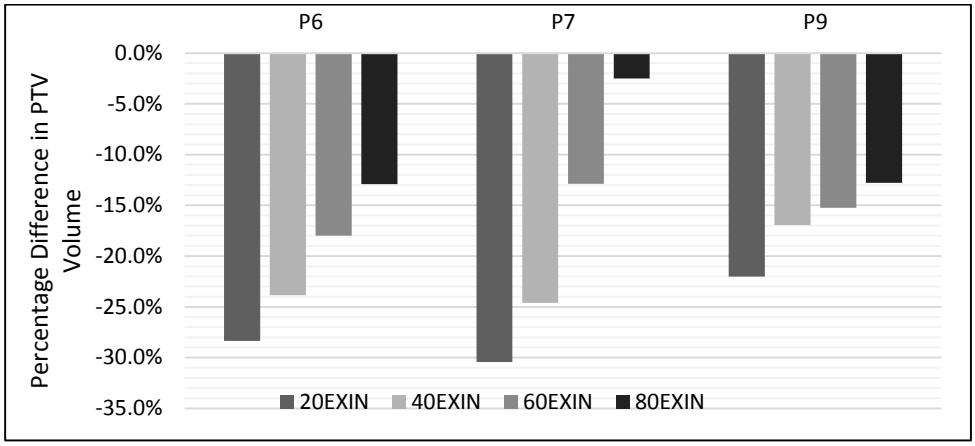

Figure 13. Percentage difference in PTV volume for the gated plans as compared to the originally non-gated plan.

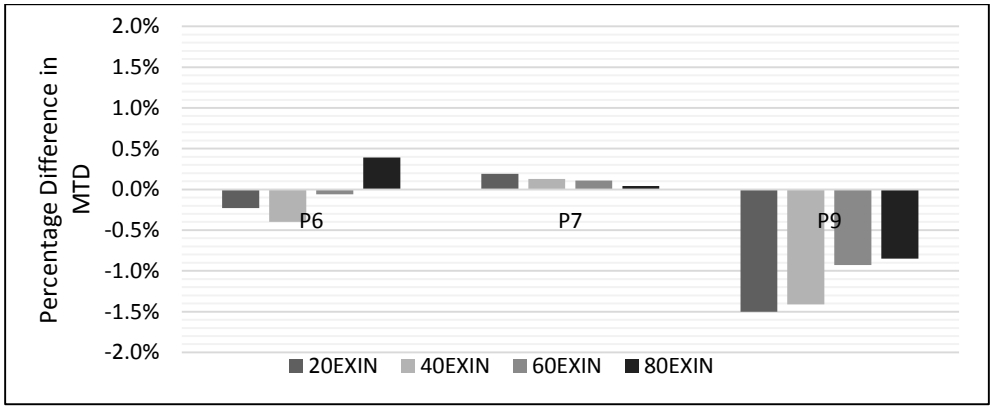

Figure 14. Percentage difference in mean tumor dose (MTD) for the gated plans as compared to the originally non-gated plan.

www.manaraa.com

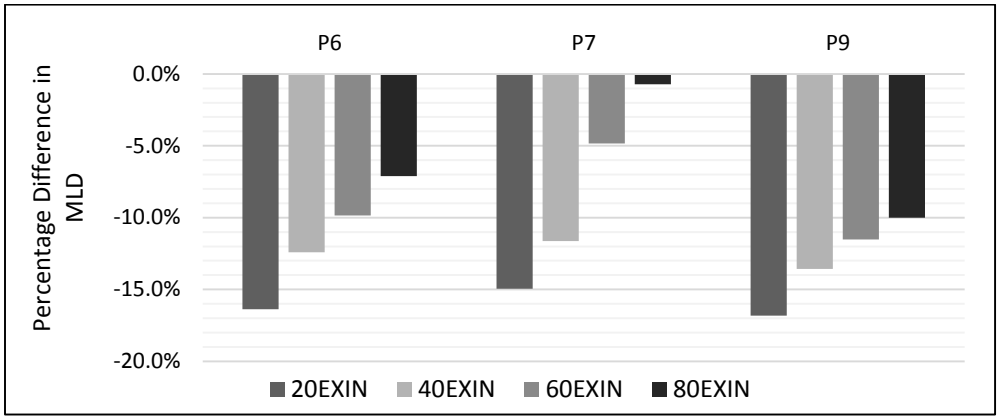

Figure 15. Percentage difference in mean lung dose (MLD) for the gated plans as compared to the originally non-gated plan.

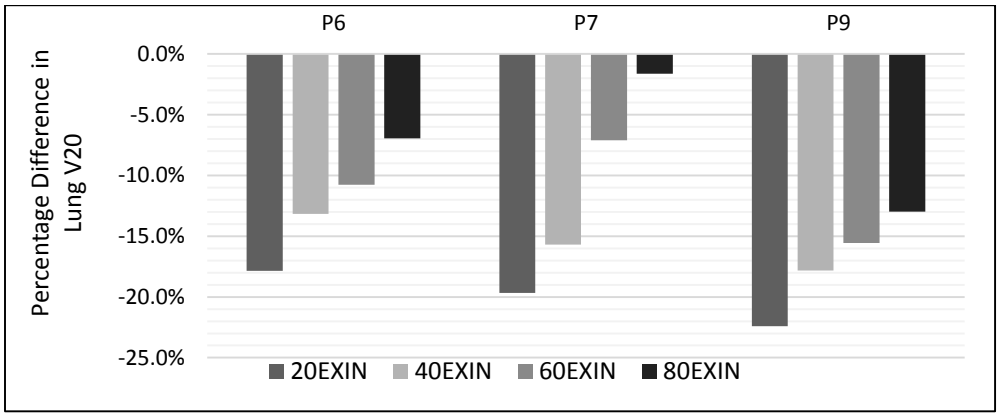

Figure 16. Percentage difference in lung V20 for the gated plans as compared to the originally non-gated plan.

www.manaraa.com

Table 4. Percentage difference between originally non-gated plans and their corresponding 20EX-20IN to 80EX-80IN gated plans.

Gating Window	Patient	PTV Volume	PTV MTD	Whole Lung MLD	Whole Lung V20	Whole Lung V10	PTV Coverage
20EX-20IN	*P6*	-28.37%	-0.23%	-16.37%	-17.84%	-17.72%	0.08%
	P7	-30.43%	0.19%	-14.96%	-19.67%	-16.72%	0.01%
	P9	-22.01%	-1.50%	-16.81%	-22.40%	-19.43%	0.02%
	Average	-26.94%	-0.51%	-16.05%	-19.97%	-17.96%	0.04%
	Standard Deviation	4.39%	0.88%	0.97%	2.29%	1.37%	0.04%
40EX-40IN	*P6*	-23.84%	-0.40%	-12.42%	-13.17%	-12.96%	0.42%
	P7	-24.62%	0.13%	-11.63%	-15.68%	-13.18%	0.04%
	P9	-16.94%	-1.41%	-13.56%	-17.83%	-15.68%	0.07%
	Average	-21.80%	-0.56%	-12.54%	-15.56%	-13.94%	0.18%
	Standard Deviation	4.23%	0.78%	0.97%	2.33%	1.51%	0.21%
60EX-60IN	*P6*	-17.99%	-0.06%	-9.84%	-10.78%	-9.46%	0.42%
	P7	-12.89%	0.11%	-4.83%	-7.10%	-6.10%	0.02%
	P9	-15.23%	-0.93%	-11.52%	-15.55%	-13.55%	0.20%
	Average	-15.37%	-0.30%	-8.73%	-11.14%	-9.70%	0.21%
	Standard Deviation	2.55%	0.56%	3.48%	4.24%	3.74%	0.20%
80EX-80IN	*P6*	-12.90%	0.39%	-7.11%	-6.95%	-7.21%	0.73%
	P7	-2.51%	0.04%	-0.73%	-1.63%	-2.31%	0.00%
	P9	-12.78%	-0.85%	-10.00%	-12.98%	-11.81%	0.23%
	Average	-9.40%	-0.14%	-5.95%	-7.18%	-7.11%	0.32%
	Standard Deviation	5.97%	0.64%	4.74%	5.68%	4.75%	0.38%

3.4.1.2 80EX-80IN Gated Patients

Table 5 summarizes the percentage differences between the 80EX-80IN gated plans and their corresponding treatment plans using reduced gating windows. For patients originally gated 80EX-80IN, the average reduction in PTV volume was -29.1±7.7%, -26.9±7.8%, and -21.3±5.2%, respectively for the 20EX-20IN to 60EX-60IN gated plans

www.manaraa.com

as compared to the 80EX-80IN gated plan (Figure 17). Differences in MTD were less than 1Gy (Figure 18), and percentage coverage was within 1% across plans for all patients. Figures 19 and 20 depict the relative percentage differences in MLD and Lung V20 across plans for each patient. MLD and Lung V20 were on average found to be reduced -5.8±1.4% and -7.0±4.3%, -4.7±0.0% and -6.0±2.9%, -4.2±0.3% and -5.4±2.1%, respectively for the 20EX-20IN to 60EX-60IN gated plans.

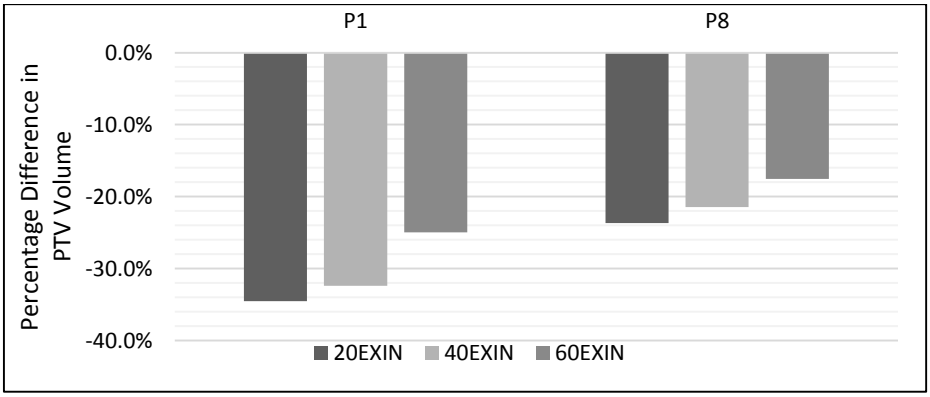

Figure 17. Percentage difference in PTV volume for the reduced gating windows as compared to the original 80EX-80IN gating.

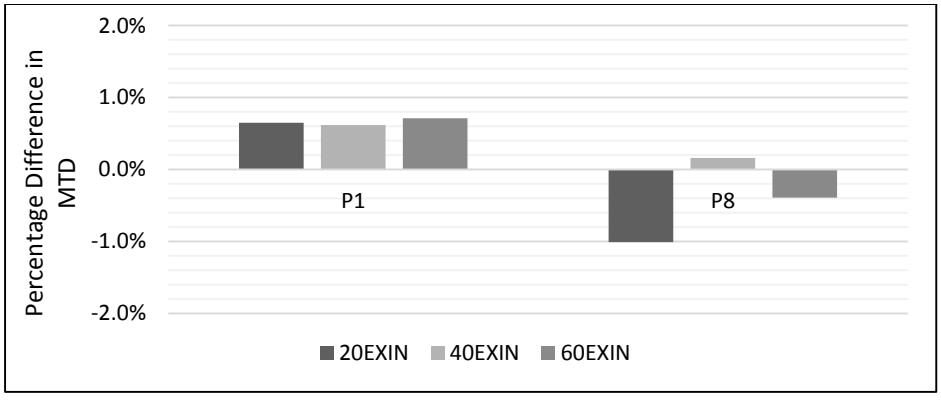

Figure 18. Percentage difference in mean tumor dose (MTD) for the reduced gating windows as compared to the original 80EX-80IN gating.

www.manaraa.com

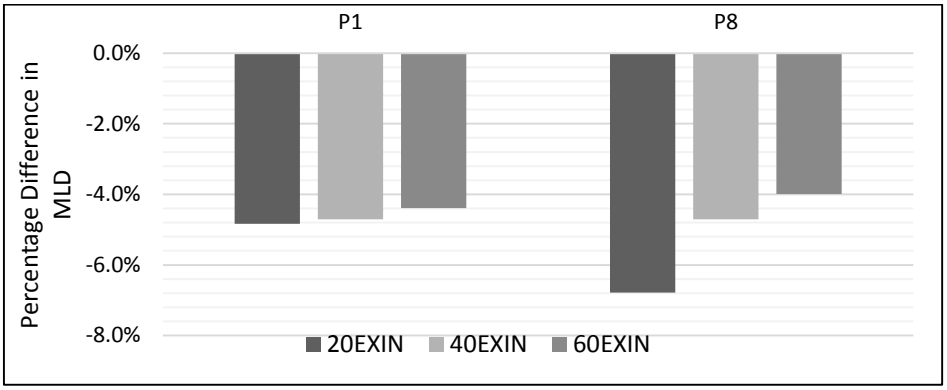

Figure 19. Percentage difference in mean lung dose (MLD) for the reduced gating windows as compared to the original 80EX-80IN gating.

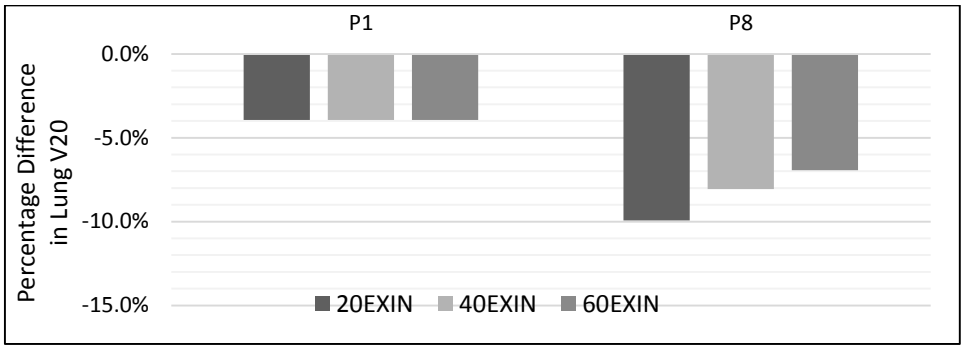

Figure 20. Percentage difference in lung V20 for the reduced gating windows as compared to the original 80EX-80IN gating.

www.manaraa.com

Table 5. Percentage difference between originally 80EX-80IN gated plans and their corresponding 20EX-20IN to 60EX-60IN gated plans.

Gating Window	Patient	PTV Volume	PTV MTD	Whole Lung MLD	Whole Lung V20	Whole Lung V10	PTV Coverage
20EX-20IN	*P1*	-34.51%	0.65%	-4.83%	-3.93%	-4.30%	0.05%
	P8	-23.67%	-1.01%	-6.78%	-9.94%	-12.21%	0.25%
	Average	-29.09%	-0.18%	-5.81%	-6.93%	-8.25%	0.15%
	Standard Deviation	7.67%	1.17%	1.38%	4.25%	5.59%	0.14%
40EX-40IN	*P1*	-32.40%	0.62%	-4.71%	-3.93%	-4.43%	-0.05%
	P8	-21.43%	0.16%	-4.71%	-8.07%	-11.03%	1.55%
	Average	-26.91%	0.39%	-4.71%	-6.00%	-7.73%	0.75%
	Standard Deviation	7.76%	0.33%	0.00%	2.93%	4.67%	1.13%
60EX-60IN	*P1*	-24.96%	0.71%	-4.39%	-3.93%	-4.43%	-0.05%
	P8	-17.56%	-0.39%	-3.99%	-6.94%	-9.15%	0.98%
	Average	-21.26%	0.16%	-4.19%	-5.43%	-6.79%	0.46%
	Standard Deviation	5.24%	0.78%	0.28%	2.12%	3.34%	0.73%

3.4.2 Treatment Time

3.4.2.1 Validation of Treatment Time Algorithm

Table 6 compares the results of the treatment time calculation algorithm with the actual treatment time obtained from the treatment records. On average, the algorithm was able to estimate treatment time within 1.1 minutes (10.7%) of the actual treatment time. In four out of five patients, the algorithm was able to predict treatment time within less than 1 minute of the actual time.

www.manaraa.com

Table 6. Validation of treatment time algorithm.

Patient	Actual Treatment Time (min)	Computed Treatment Time (min)	Absolute Difference (min)	Percent Difference (%)
1	7.6	8.0	0.4	5.3
6	5.5	5.3	0.2	3.6
7	11.7	8.0	3.7	31.6
8	5.0	5.2	0.2	4.0
9	9.0	8.2	0.8	8.9
		Average	1.1	10.7
		Standard Deviation	1.5	11.9

3.4.2.2 Non-gated Patients

Figure 21 depicts the percentage difference in treatment times between the non-gated plans and their corresponding 20EX-20IN to 80EX-80IN gated plans. Treatment delivery times are listed in Table 7. When using a dose rate of 500Mu/min for both the non-gated and gated plans, treatment delivery times were on average found to increase 29.0±21.3% (3.2±2.9min), 18.5±15.0% (2.0±2.0min), 10.2±11.0% (1.1±1.4min), and 4.9±7.1% (0.6±0.9min), respectively.

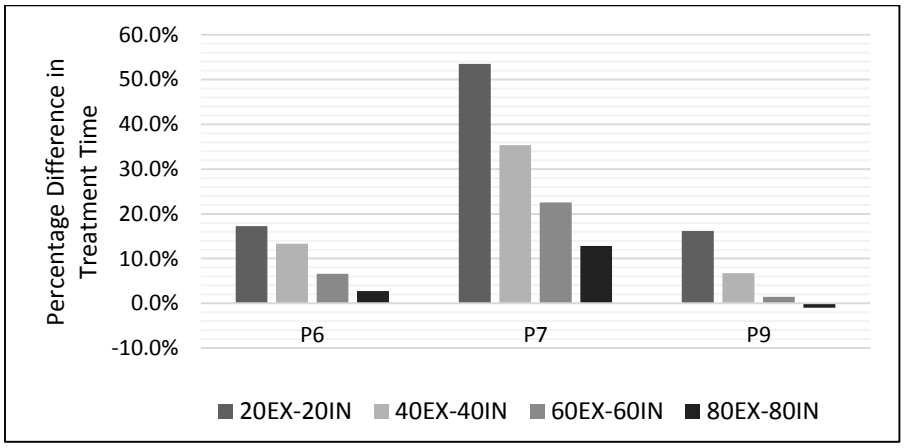

Figure 21. Percentage difference in treatment time for the gated plans as compared to the originally non-gated plan when using a dose rate of 500MU/min.

www.manaraa.com

Table 7. Treatment time difference between originally non-gated plans and their corresponding 20EX-20IN to 80EX-80IN gated plans using dose rate = 500MU/min.

Patient	Gating Window	Treatment Time 500MU/min	Percentage Difference in time from Non-gated Plan	Absolute Difference in time from Non-gated Plan
P6	*Non-gated*	7.77258	-	-
	20EX-20IN	9.11156	17.23%	1.34
	40EX-40IN	8.81029	13.35%	1.04
	60EX-60IN	8.28339	6.57%	0.51
	80EX-80IN	7.98724	2.76%	0.21
P7	*Non-gated*	12.18083	-	-
	20EX-20IN	18.69779	53.50%	6.52
	40EX-40IN	16.48543	35.34%	4.30
	60EX-60IN	14.92953	22.57%	2.75
	80EX-80IN	13.74399	12.83%	1.56
P9	*Non-gated*	9.92172	-	-
	20EX-20IN	11.52439	16.15%	1.60
	40EX-40IN	10.59479	6.78%	0.67
	60EX-60IN	10.06525	1.45%	0.14
	80EX-80IN	9.82761	-0.95%	-0.09

Treatment times were next compared using an increased dose rate for the gated plans. Dose rate for the non-gated plans was kept at 500MU/min, while dose rate for the 20EX-20IN to 80EX-80IN gated plans was raised to 1500Mu/min. Figure 22 and Table 8 outline these results. By increasing the dose rate for the gated plans, treatment times were found to be reduced compared to the original non-gated plans, with larger gating windows requiring less time than smaller windows. On average, treatment delivery times were found to decrease -19.7±7.0% (-1.9±0.4min), -22.7±5.5% (-2.2±0.6min), -25.5.2±6.0% (-2.5±0.8min), and -27.2±6.6% (-2.7±0.9min), respectively.

www.manaraa.com

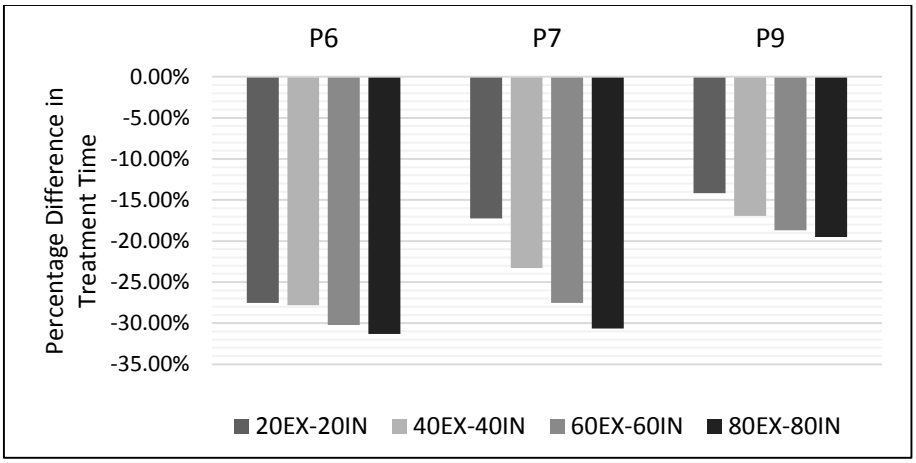

Figure 22. Percentage difference in treatment time for gated plans using a dose rate of 1500MU/min as compared to the originally non-gated plan using a dose rate of 500MU/min.

Table 8. Treatment time difference between originally non-gated plans (dose rate = 500MU/min) and their corresponding 20EX-20IN to 80EX-80IN gated plans (dose rate = 1500MU/min).

Patient	Gating Window	Treatment Time 500 MU/min vs. 1500MU/min	Percentage Difference in time from Non-gated Plan	Absolute Difference in time from Non-gated Plan
P6	*Non-gated*	7.77258	-	-
	20EX-20IN	5.63347	-27.52%	-2.14
	40EX-40IN	5.61098	-27.81%	-2.16
	60EX-60IN	5.42491	-30.20%	-2.35
	80EX-80IN	5.33908	-31.31%	-2.43
P7	*Non-gated*	12.18083	-	-
	20EX-20IN	10.07971	-17.25%	-2.10
	40EX-40IN	9.34226	-23.30%	-2.84
	60EX-60IN	8.82696	-27.53%	-3.35
	80EX-80IN	8.44888	-30.64%	-3.73
P9	*Non-gated*	9.92172	-	-
	20EX-20IN	8.51439	-14.18%	-1.41
	40EX-40IN	8.24163	-16.93%	-1.68
	60EX-60IN	8.06579	-18.71%	-1.86
	80EX-80IN	7.98657	-19.50%	-1.94

www.manaraa.com

3.4.2.3 80EX-80IN Gated Patients

Figure 23 depicts the percentage difference in treatment time between treatment plans originally gated 80EX-80IN and their corresponding 20EX-20IN to 60EX-60IN gated plans. Treatment delivery times are listed in Table 9. When using a dose rate of 500MU/min for both the original and smaller gated plans, treatment delivery times were on average found to increase 16.9±23.4% (1.0±1.4min), 4.9±12.8% (0.3±0.8min), and 4.6±0.9% (0.3±0.1min), respectively. Patient 8 did not exhibit the same pattern as seen in the remaining patients (smaller gating windows require more time), and instead had relatively similar treatment times across the four gated plans. This is likely due to this patient spending a majority of the breathing cycle in the full exhalation phase (0EX) of respiration, thereby giving similar gating factors for the 20EX-20IN (60%), 40EX-40IN (70%), 60EX-60IN (78%), and 80EX-80IN (89%) gating windows. Further investigation also noted that for this patient, the mechanical time took longer for the 60EX-60IN (87sec) and 80EX-80IN (82sec) gating windows than for the 20EX-20IN (69sec) and 40EX-40IN (63sec) gating windows. The combination of similar gating factors and shorter mechanical times for the smaller gating windows allowed for comparable treatment times across the 20EX-20IN to 80EX-80IN gated plans.

www.manaraa.com

Table 9. Treatment time difference between plans originally gated 80EX-80IN and their corresponding 20EX-20IN to 60EX-60IN gated plans using dose rate = 500MU/min.

Patient	Gating Window	Treatment Time 500 MU/min vs. 1500MU/min	Percentage Difference in time from Non-gated Plan	Absolute Difference in time from Non-gated Plan
P1	*80EX-80IN*	6.15216	-	-
	20EX-20IN	8.2111	33.47%	2.06
	40EX-40IN	7.00859	13.92%	0.86
	60EX-60IN	6.47387	5.23%	0.32
P8	*80EX-80IN*	5.2218	-	-
	20EX-20IN	5.24185	0.38%	0.02
	40EX-40IN	5.00652	-4.12%	-0.22
	60EX-60IN	5.43157	4.02%	0.21

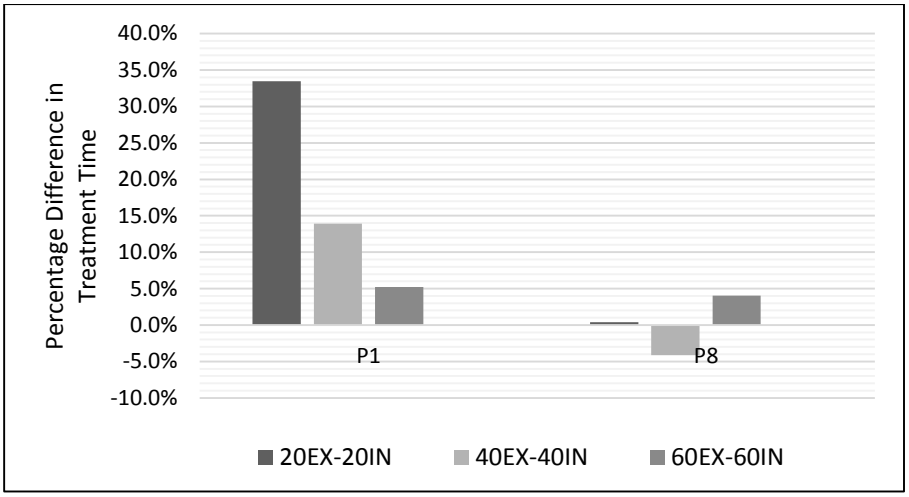

Figure 23. Percentage difference in treatment time for the gated plans as compared to the original 80EX-80IN gated plan when using a dose rate of 500MU/min. Patient 8 had relatively similar treatment times across the four gated plans. This is likely due to the combination of similar gating factors and shorter mechanical times for the smaller gating windows, which allowed for comparable treatment times across the 20EX-20IN to 80EX-80IN gated plans.

Treatment times were next compared using an increased dose rate of 1500MU/min for the 20EX-20IN to 60EX-60IN gated plans, while keeping the original

www.manaraa.com

80EX-80IN gated plan at 500MU/min. Figure 24 and Table 10 outline these results. By increasing the dose rate for the gated plans, treatment times were on average found to be reduced -15.6±5.2% (-0.9±0.4min), -20.3±7.9% (-1.2±0.6min), and -17.7±15.5% (-1.1±1.0min), respectively. In the case of P8, the 60EX-60IN gated plan took longer to deliver than the 20EX-20IN and 40EX-40IN gated plans. This likely again due to the combination of similar gating factors and shorter mechanical times required for the 20EX-20IN and 40EX-40IN gated plans as compared to the 60EX-60IN gated.

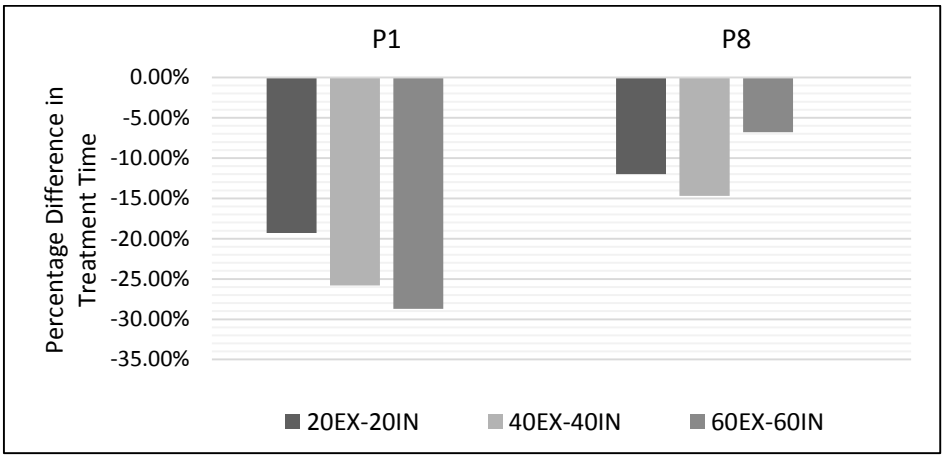

Figure 24. Percentage difference in treatment time for gated plans using a dose rate of 1500MU/min as compared to the original 80EX-80IN gated plan using a dose rate of 500Mu/min. In the case of P8, the 60EX-60IN gated plan took longer to deliver than the 20EX-20IN and 40EX-40IN gated plans. This likely due to the combination of similar gating factors and shorter mechanical times required for the 20EX-20IN and 40EX-40IN gated plans as compared to the 60EX-60IN gated plan.

.

www.manaraa.com

Table 10. Treatment time difference between plans originally gated 80EX-80IN (dose rate = 500MU/min).and their corresponding 20EX-20IN to 60EX-60IN gated plans (dose rate = 1500MU/min).

Patient	Gating Window	Treatment Time 500 MU/min vs. 1500MU/min	Percentage Difference in time from Non-gated Plan	Absolute Difference in time from Non-gated Plan
P1	*80EX-80IN*	6.15216	-	-
	20EX-20IN	4.96507	-19.30%	-1.19
	40EX-40IN	4.56423	-25.81%	-1.59
	60EX-60IN	4.38599	-28.71%	-1.77
P8	*80EX-80IN*	5.2218	-	-
	20EX-20IN	4.59569	-11.99%	-0.63
	40EX-40IN	4.45392	-14.71%	-0.77
	60EX-60IN	4.86749	-6.79%	-0.35

3.5 Discussion

As has been demonstrated in previous respiratory gated radiation therapy studies [25, 26, 36, 37], the planning target volume for all patients could be reduced, indicating a smaller total volume received the target dose. The PTV coverage and mean tumor dose were able to be maintained, suggesting that the target was just as effectively able to be treated. Furthermore, mean lung dose and lung V20 were shown to decrease (Tables 4 and 5) when smaller gating windows were selected, implying toxicity to the whole lung was decreased. For the smallest gating window, 20EX-20IN, MLD was on average reduced by -16.1±1.0% in originally non-gated plans and by -5.8±1.4% in plans originally gated 80EX-80IN- an absolute difference of -87.9±19.9 cGy and -46.7±48.8 cGy, respectively. Likewise, lung V20 was on average reduced by -20.0±2.3% in originally non-gated plans and by -6.9±4.3% in plans originally gated 80EX-80IN- an absolute difference of -1.5±0.1% and -1.0±1.2%, respectively. Some authors [27, 36] have pointed out that respiratory gating studies such as ours, evaluate the dosimetric

www.manaraa.com

benefits of respiratory gating, and whether these findings directly transfer to a successful patient outcome is unknown. However, MLD and lung V20 have been proposed as predictive factors for radiation pneumonitis [41, 42] and are often used clinically as dose constraints. Though no studies have directly evaluated the effects of respiratory gating on radiation pneumonitis, results of these dosimetric studies imply that respiratory gating can reduce the risk of radiation pneumonitis. When selecting patients for respiratory gating and choosing appropriate gating windows, the dosimetric benefits of gated treatment should be weighed along with the clinical risk for radiation pneumonitis.

One of the most commonly cited disadvantages of respiratory gated radiation therapy is the increased time for treatment delivery and, consequently, the increased potential for uncertainty introduced from patient movement. In order to compare the temporal effects of respiratory gating, we developed an algorithm for estimating the corresponding delivery time for each treatment plan. To validate this algorithm, computed delivery times were compared against actual treatment times as obtained from the treatment record. In four out of five patients, the algorithm was able to predict treatment time within less than 1 minute of the actual time. While these results suggest that the algorithm is able to provide an estimate for treatment time, we recognize that a larger sample size should be tested in order to provide further validation.

Reviewing the treatment time data (Figures 21-24) smaller gating windows were shown to require longer delivery times when dose rate was unchanged. However, since patients are known to spend the majority of breathing time in the exhalation phases of respiration, increase in time required was not linearly proportional to the number of respiratory phases within the gating window. For example, the 20EX-20IN gating

www.manaraa.com

window includes three respiratory phases (20EX, 0EX, 20IN), while the 80EX-80IN gating window includes nine respiratory phases (80EX, 60EX, 40EX, 20EX, 0EX, 20IN, 40IN, 60IN, 80IN), though, as we see Figure 25, patients did not spend three times longer in the 80EX-80IN window as they did in the 20EX-20IN window, but rather spent more than half of the breathing cycle within the 20EX-20IN window. Because of this relationship, increase in time due to gating was only a fraction of the non-gated time. The 20EX-20IN window was estimated to have the greatest increase in delivery time: 29.0±21.3% percent on average, corresponding to an absolute difference of 3.2±2.9 minutes, while the 80EX-80IN gating window was on average only found to increase time 4.9±7.1%, an absolute difference of 0.6±0.9 minutes. When selecting patients for respiratory gating and choosing appropriate gating windows, patient compliance is another important factor that should be considered, and techniques such as additional breath coaching may be introduced to minimize the potential for errors. For patients with good compliance, an increase of time within these magnitudes may not pose a major burden, though this should be assessed on an individual basis. Prolonged treatment times for respiratory gating may be reduced by increasing the dose rate. As can be seen in Figure 22, raising the dose rate from 500 MU/min to 1500 MU/min was shown to decrease delivery time to even less than the time taken for non-gated treatment.

www.manaraa.com

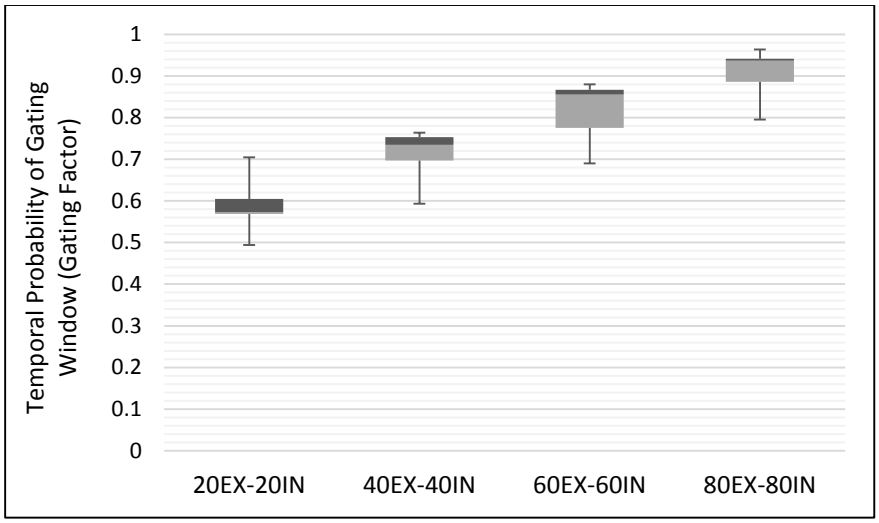

Figure 25. Temporal probability for the 20EX-20IN to 80EX-80IN gating windows. These gating factors were used to scale delivery time for the gated treatments.

The biggest limitation to this study was the small patient sample size (n=5), which was made smaller by separating patients that had been treated using 80EX-80IN gated treatment (n=2), from those that had undergone non-gated treatment (n=3). One drawback to this constraint is that we were unable to investigate parameters predicting the potential benefits of respiratory gating. For example, Jang *et al.* noted that dosimetric benefits were achieved with respiratory gating for highly mobile lung tumors (3D mobility >10 mm), as well as with tumors with low mobility and a small GTV, but not in the case of tumors with low mobility and a large GTV (GTV_{eoe} > 10cc). [25] The next step in this research will be to repeat this study using a larger patient sample size, and assess whether we find these same predictive factors to hold true. Additionally, an increased sample size will allow us to further validate the treatment time calculation algorithm, as well as determine factors that have the largest impact on delivery time.

www.manaraa.com

In summary, respiratory gated radiation therapy in lung cancer patients was shown to reduce lung toxicity, while maintaining mean tumor dose and PTV coverage. Additionally, increased dose rates were shown to achieve treatment delivery times comparable to or faster than non-gated delivery times. When selecting patients for respiratory gating and choosing appropriate gating windows, the dosimetric benefits of gated treatment should be considered along with the clinical risks of treatment and the patient's ability to comply.

www.manaraa.com

CHAPTER 4: CONCLUSION

We examined two practices in which 4DCT is used in radiotherapy treatment planning for lung cancer. In our first study, we compared 3-Dimensional (3D) dose calculation using a conventional breath-hold CT to 4-Dimensional (4D) dose calculation using 4DCT, and investigated the dosimetric uncertainty in 4D dose calculation using three different temporal probability distributions: uniform distribution, sinusoidal distribution, and patient-specific distribution derived from the patient's respiratory trace. We found that conventional 3D dose calculation may overestimate lung V20 (volume of the lung receiving more than 20Gy), mean lung dose, and mean tumor dose, though, the absolute difference between 3D and 4D dose calculation in lung tumors may not be clinically significant. Furthermore, we concluded that 4D dose computed using either a uniform or sinusoidal temporal probability distribution is able to approximate 4D dose computed using the patient-specific respiratory trace.

Our second study evaluated the dosimetric and temporal effects of respiratory gated radiation therapy using four different gating windows and estimated the corresponding treatment delivery times for normal (500MU/min) and high (1500MU/min) dose rates. Our results showed that gated radiation therapy in lung cancer patients could potentially reduce lung toxicity, while just as effectively treating the target volume. Though reducing the gating window prolonged the treatment time, increased dose rates were shown to achieve treatment delivery times comparable to or faster than non-gated delivery times.

In the future, it would be advantageous to repeat these studies using a larger patient sample size in order to assess whether certain predictive factors such as the

www.manaraa.com

magnitude of tumor motion or the size of the gating window may correlate to the accuracy of the approximated 4D dose volume, in the case of the first study, or the potential benefits of respiratory gating, in the case of the second study.

www.manaraa.com

APPENDIX A: 4D DOSE CALCULATION TABLES

Table A-1. Lung V20 Values.

Patient	Lung V20 3D (%)	Lung V20 4D Patient-Specific Weighting (%)	Lung V20 4D Uniform Weighting (%)	Lung V20 4D Sine Weighting (%)
1	8.03	7.07	7.57	7.35
2	41.96	46.14	45.38	45.86
3 (LT)	20.98	18.62	18.67	18.66
3 (RT)	7.83	7.13	6.95	7.06
4	64.18	65.16	64.69	64.78
5	64.34	61.70	61.72	61.73
6	15.75	15.23	15.27	15.27
7	17.82	14.37	14.58	14.44
8	45.73	45.39	45.22	45.23
9	15.37	14.50	14.07	14.05

Table A-2. Lung V20 Percent Difference from 4D Dose Calculation Using Patient-Specific Weighting.

Patient	Lung V20 3D (%)	Lung V20 4D Uniform Weighting (%)	Lung V20 4D Sine Weighting (%)
1	13.58%	7.07%	3.96%
2	-9.06%	-1.65%	-0.61%
3 (LT)	12.67%	0.27%	0.21%
3 (RT)	9.82%	-2.52%	-0.98%
4	-1.50%	-0.72%	-0.58%
5	4.28%	0.03%	0.05%
6	3.41%	0.26%	0.26%
7	24.01%	1.46%	0.49%
8	0.75%	-0.37%	-0.35%
9	6.00%	-2.97%	-3.10%
Average	6.40%	0.09%	-0.07%
Standard Deviation	9.19%	2.80%	1.75%

www.manaraa.com

Table A-3. Lung V20 Percent Difference from 3D Dose Calculation.

Patient	Lung V20 4D Patient-Specific Weighting (%)	Lung V20 4D Uniform Weighting (%)	Lung V20 4D Sine Weighting (%)
1	-11.96%	-5.73%	-8.47%
2	9.96%	8.15%	9.29%
3 (LT)	-11.25%	-11.01%	-11.06%
3 (RT)	-8.94%	-11.24%	-9.83%
4	1.53%	0.79%	0.93%
5	-4.10%	-4.07%	-4.06%
6	-3.30%	-3.05%	-3.05%
7	-19.36%	-18.18%	-18.97%
8	-0.74%	-1.12%	-1.09%
9	-5.66%	-8.46%	-8.59%
Average	-5.38%	-5.39%	-5.49%
Standard Deviation	8.14%	7.35%	7.73%

Table A-4. Mean Tumor Dose Values.

Patient	MTD 3D (Gy)	MTD 4D Patient-Specific Weighting (Gy)	MTD 4D Uniform Weighting (Gy)	MTD 4D Sine Weighting (Gy)
1	49.79	49.16	49.38	49.25
2	72.27	70.20	70.58	70.36
3 (LT)	56.69	56.15	55.95	56.07
3 (RT)	57.87	57.51	57.49	57.52
4	66.03	65.85	65.27	65.24
5	29.44	29.69	29.62	29.62
6	42.62	42.21	42.23	42.23
7	60.49	58.12	58.67	58.21
8	64.32	63.45	62.89	63.05
9	45.10	45.00	44.74	44.68

www.manaraa.com

Table A-5. Mean Tumor Dose Percent Difference from 4D Dose Calculation Using Patient-Specific Weighting.

Patient	MTD 3D (%)	MTD 4D Uniform Weighting (%)	MTD 4D Sine Weighting (%)
1	1.28%	0.45%	0.18%
2	2.95%	0.54%	0.23%
3 (LT)	0.96%	-0.36%	-0.14%
3 (RT)	0.63%	-0.03%	0.02%
4	0.27%	-0.88%	-0.93%
5	-0.84%	-0.24%	-0.24%
6	0.97%	0.05%	0.05%
7	4.08%	0.95%	0.15%
8	1.37%	-0.88%	-0.63%
9	0.22%	-0.58%	-0.71%
Average	1.19%	-0.10%	-0.20%
Standard Deviation	1.41%	0.61%	0.41%

Table A-6. Mean Tumor Dose Percent Difference from 3D Dose Calculation.

Patient	MTD 4D Patient-Specific Weighting (%)	MTD 4D Uniform Weighting (%)	MTD 4D Sine Weighting (%)
1	-1.27%	-0.82%	-1.08%
2	-2.86%	-2.34%	-2.64%
3 (LT)	-0.95%	-1.31%	-1.09%
3 (RT)	-0.62%	-0.66%	-0.60%
4	-0.27%	-1.15%	-1.20%
5	0.85%	0.61%	0.61%
6	-0.96%	-0.92%	-0.92%
7	-3.92%	-3.01%	-3.77%
8	-1.35%	-2.22%	-1.97%
9	-0.22%	-0.80%	-0.93%
Average	-1.16%	-1.26%	-1.36%
Standard Deviation	1.36%	1.03%	1.19%

www.manaraa.com

Table A-7. Mean Lung Dose.

Patient	MLD 3D (Gy)	MLD 4D Patient-Specific Weighting (Gy)	MLD 4D Uniform Weighting (Gy)	MLD 4D Sine Weighting (Gy)
1	4.76	4.53	4.73	4.65
2	23.56	25.00	24.67	24.86
3 (LT)	13.14	11.99	11.94	11.98
3 (RT)	8.16	7.79	7.66	7.74
4	35.01	35.15	34.59	34.60
5	22.66	22.17	22.13	22.14
6	9.38	9.30	9.31	9.32
7	9.52	7.57	7.66	7.60
8	23.18	22.69	22.51	22.57
9	10.10	9.71	9.50	9.50

Table A-8. Mean Lung Dose Percent Difference from 4D Dose Calculation Using Patient-Specific Weighting.

Patient	MLD 3D (%)	MLD 4D Uniform Weighting (%)	MLD 4D Sine Weighting (%)
1	5.08%	4.42%	2.65%
2	-5.76%	-1.32%	-0.56%
3 (LT)	9.59%	-0.42%	-0.08%
3 (RT)	4.75%	-1.67%	-0.64%
4	-0.40%	-1.59%	-1.56%
5	2.21%	-0.18%	-0.14%
6	0.86%	0.11%	0.22%
7	25.76%	1.19%	0.40%
8	2.16%	-0.79%	-0.53%
9	4.02%	-2.16%	-2.16%
Average	4.83%	-0.24%	-0.24%
Standard Deviation	8.37%	1.91%	1.28%

www.manaraa.com

Table A-9. Mean Tumor Dose Percent Difference from 3D Dose Calculation.

Patient	MLD 4D Patient-Specific Weighting (%)	MLD 4D Uniform Weighting (%)	MLD 4D Sine Weighting (%)
1	-4.83%	-0.63%	-2.31%
2	6.11%	4.71%	5.52%
3 (LT)	-8.75%	-9.13%	-8.83%
3 (RT)	-4.53%	-6.13%	-5.15%
4	0.40%	-1.20%	-1.17%
5	-2.16%	-2.34%	-2.29%
6	-0.85%	-0.75%	-0.64%
7	-20.48%	-19.54%	-20.17%
8	-2.11%	-2.89%	-2.63%
9	-3.86%	-5.94%	-5.94%
Average	-4.11%	-4.38%	-4.36%
Standard Deviation	6.94%	6.53%	6.72%

www.manaraa.com

Table A-10. Gamma Values (PTV Region).

Patient	Gamma 4D Uniform Weighting (%)	Gamma 4D Sine Weighting (%)
1	100.00%	100.00%
2	99.12%	99.88%
3 (LT)	100.00%	100.00%
3 (RT)	100.00%	100.00%
4	99.93%	99.58%
5	99.86%	99.78%
6	100.00%	100.00%
7	100.00%	100.00%
8	98.41%	99.99%
9	99.94%	99.92%
Average	99.73%	99.92%
Standard Deviation	0.54%	0.14%

Table A-11. Gamma Values (Lung Region).

Patient	Gamma 4D Uniform Weighting (%)	Gamma 4D Sine Weighting (%)
1	99.99%	100.00%
2	99.26%	99.88%
3 (LT)	99.92%	99.92%
3 (RT)	99.98%	100.00%
4	97.73%	97.39%
5	99.98%	99.99%
6	99.95%	99.94%
7	100.00%	100.00%
8	99.34%	99.90%
9	99.93%	99.82%
Average	99.61%	99.68%
Standard Deviation	0.72%	0.81%

www.manaraa.com

APPENDIX B: GATED RADIATION THERAPY TABLES

Table B-1. Dosimetric difference between originally non-gated plans and their corresponding 20EX-20IN to 80EX-80IN gated plans.

Gating Window	Patient	PTV Volume (cm^3)	PTV MTD (cGy)	Whole Lung MLD (cGy)	Whole Lung V20 (%)	Whole Lung V10 (%)	PTV Coverage (%)
P6	*Non-gated*	109.419	4262.2	574.2	8.35%	19.13%	96.77%
	20EX-20IN	78.3746	4252.2	480.2	6.86%	15.74%	96.85%
	40EX-40IN	83.3354	4245	502.9	7.25%	16.65%	97.18%
	60EX-60IN	89.7375	4259.8	517.7	7.45%	17.32%	97.18%
	80EX-80IN	95.3030	4278.8	533.4	7.77%	17.75%	97.48%
P7	*Non-gated*	33.1885	6081.2	438.5	6.76%	12.14%	93.71%
	20EX-20IN	23.0882	6092.6	372.9	5.43%	10.11%	93.72%
	40EX-40IN	25.0175	6088.9	387.5	5.70%	10.54%	93.75%
	60EX-60IN	28.9113	6087.6	417.3	6.28%	11.40%	93.73%
	80EX-80IN	32.3559	6083.9	435.3	6.65%	11.86%	93.71%
P9	*Non-gated*	141.318	4550.1	618.7	7.01%	18.37%	96.21%
	20EX-20IN	110.207	4482	514.7	5.44%	14.80%	96.23%
	40EX-40IN	117.380	4486.1	534.8	5.76%	15.49%	96.28%
	60EX-60IN	119.793	4507.6	547.4	5.92%	15.88%	96.40%
	80EX-80IN	123.252	4511.3	556.8	6.10%	16.20%	96.43%

Table B-2. Dosimetric difference between originally 80EX-80IN gated plans and their corresponding 20EX-20IN to 60EX-60IN gated plans.

Gating Window	Patient	PTV Volume (cm^3)	PTV MTD (cGy)	Whole Lung MLD (cGy)	Whole Lung V20 (%)	Whole Lung V10 (%)	PTV Coverage (%)
P1	*80EX-80IN*	14.1277	5157.8	252.7	4.07%	7.68%	99.16%
	20EX-20IN	9.25254	5191.3	240.5	3.91%	7.35%	99.21%
	40EX-40IN	9.55008	5190	240.8	3.91%	7.34%	99.11%
	60EX-60IN	10.601	5194.6	241.6	3.91%	7.34%	99.11%
P8	*80EX-80IN*	114.574	6432.9	1197	19.32%	24.58%	97.23%
	20EX-20IN	87.4571	6368.1	1115.8	17.40%	21.58%	97.47%
	40EX-40IN	90.0246	6443.2	1140.6	17.76%	21.87%	98.74%
	60EX-60IN	94.4569	6407.5	1149.2	17.98%	22.33%	98.18%

www.manaraa.com

Table B-3. Treatment time difference between for patients originally non-gated and their corresponding 20EX-20IN to 80EX-80IN gated plans.

Patient	Gating Window	Gating Factor	Treatment Time 500MU/min	Treatment Time 1500MU/min	Reduction in Time from 500MU/min to 1500Mu/min
P6	*Non-gated*	1	7.77258	5.31258	31.65%
	20EX-20IN	0.7046	9.11156	5.63347	38.17%
	40EX-40IN	0.7635	8.81029	5.61098	36.31%
	60EX-60IN	0.855	8.28339	5.42491	34.51%
	80EX-80IN	0.9365	7.98724	5.33908	33.15%
P7	*Non-gated*	1	12.18083	7.98883	34.41%
	20EX-20IN	0.494	18.69779	10.07971	46.09%
	40EX-40IN	0.5932	16.48543	9.34226	43.33%
	60EX-60IN	0.6902	14.92953	8.82696	40.88%
	80EX-80IN	0.7952	13.74399	8.44888	38.53%
P9	*Non-gated*	1	9.92172	8.15906	17.77%
	20EX-20IN	0.5732	11.52439	8.51439	26.12%
	40EX-40IN	0.7349	10.59479	8.24163	22.21%
	60EX-60IN	0.8669	10.06525	8.06579	19.86%
	80EX-80IN	0.9415	9.82761	7.98657	18.73%

Table B-4. Treatment time difference for patients originally gated 80EX-80IN and their corresponding 20EX-20IN to 60EX-60IN gated plans.

Patient	Gating Window	Gating Factor	Treatment Time 500MU/min	Treatment Time 1500MU/min	Reduction in Time from 500MU/min to 1500Mu/min
P1	*80EX-80IN*	0.9635	6.15216	4.2812	30.41%
	20EX-20IN	0.5689	8.2111	4.96507	39.53%
	40EX-40IN	0.7533	7.00859	4.56423	34.88%
	60EX-60IN	0.88	6.47387	4.38599	32.25%
P8	*80EX-80IN*	0.8862	5.2218	4.74034	9.22%
	20EX-20IN	0.6046	5.24185	4.59569	12.33%
	40EX-40IN	0.6973	5.00652	4.45392	11.04%
	60EX-60IN	0.7753	5.43157	4.86749	10.39%

www.manaraa.com

REFERENCES

1. Society, A.C., *Cancer Facts & Figures 2014.* 2014.
2. Murshed, H., et al., *Dose and volume reduction for normal lung using intensity-modulated radiotherapy for advanced-stage non-small-cell lung cancer.* Int J Radiat Oncol Biol Phys, 2004. **58**(4): p. 1258-67.
3. Simone, C.B., 2nd, et al., *Stereotactic body radiation therapy for lung cancer.* Chest, 2013. **143**(6): p. 1784-90.
4. Wulf, J., et al., *Dose-response in stereotactic irradiation of lung tumors.* Radiother Oncol, 2005. **77**(1): p. 83-7.
5. Liu, H.H., et al., *Feasibility of sparing lung and other thoracic structures with intensity-modulated radiotherapy for non-small-cell lung cancer.* Int J Radiat Oncol Biol Phys, 2004. **58**(4): p. 1268-79.
6. Keall, P.J., et al., *The management of respiratory motion in radiation oncology report of AAPM Task Group 76.* Med Phys, 2006. **33**(10): p. 3874-900.
7. Shimizu, S., et al., *Impact of respiratory movement on the computed tomographic images of small lung tumors in three-dimensional (3D) radiotherapy.* Int J Radiat Oncol Biol Phys, 2000. **46**(5): p. 1127-33.
8. Seppenwoolde, Y., et al., *Precise and real-time measurement of 3D tumor motion in lung due to breathing and heartbeat, measured during radiotherapy.* Int J Radiat Oncol Biol Phys, 2002. **53**(4): p. 822-34.
9. Guckenberger, M., et al., *Is a single respiratory correlated 4D-CT study sufficient for evaluation of breathing motion?* Int J Radiat Oncol Biol Phys, 2007. **67**(5): p. 1352-9.
10. de Koste, J.R., et al., *Are multiple CT scans required for planning curative radiotherapy in lung tumors of the lower lobe?* Int J Radiat Oncol Biol Phys, 2003. **55**(5): p. 1394-9.
11. Shirato, H., et al., *Intrafractional tumor motion: lung and liver.* Semin Radiat Oncol, 2004. **14**(1): p. 10-8.
12. Mageras, G.S., et al., *Measurement of lung tumor motion using respiration-correlated CT.* Int J Radiat Oncol Biol Phys, 2004. **60**(3): p. 933-41.
13. Guckenberger, M., et al., *Four-dimensional treatment planning for stereotactic body radiotherapy.* Int J Radiat Oncol Biol Phys, 2007. **69**(1): p. 276-85.
14. Rietzel, E., et al., *Four-dimensional image-based treatment planning: Target volume segmentation and dose calculation in the presence of respiratory motion.* Int J Radiat Oncol Biol Phys, 2005. **61**(5): p. 1535-50.
15. Wu, J., et al., *An evaluation of planning techniques for stereotactic body radiation therapy in lung tumors.* Radiother Oncol, 2008. **87**(1): p. 35-43.
16. Wang, L., et al., *Dosimetric comparison of stereotactic body radiotherapy using 4D CT and multiphase CT images for treatment planning of lung cancer:*

www.manaraa.com

evaluation of the impact on daily dose coverage. Radiother Oncol, 2009. **91**(3): p. 314-24.

17. Keall, P., *4-dimensional computed tomography imaging and treatment planning.* Semin Radiat Oncol, 2004. **14**(1): p. 81-90.
18. Underberg, R.W., et al., *Four-dimensional CT scans for treatment planning in stereotactic radiotherapy for stage I lung cancer.* Int J Radiat Oncol Biol Phys, 2004. **60**(4): p. 1283-90.
19. Rietzel, E., et al., *Design of 4D treatment planning target volumes.* Int J Radiat Oncol Biol Phys, 2006. **66**(1): p. 287-95.
20. Flampouri, S., et al., *Estimation of the delivered patient dose in lung IMRT treatment based on deformable registration of 4D-CT data and Monte Carlo simulations.* Phys Med Biol, 2006. **51**(11): p. 2763-79.
21. Sura, S., et al., *Intensity-modulated radiation therapy (IMRT) for inoperable non-small cell lung cancer: the Memorial Sloan-Kettering Cancer Center (MSKCC) experience.* Radiother Oncol, 2008. **87**(1): p. 17-23.
22. Khan, F.M., *The physics of radiation therapy*. 3rd ed. 2003, Philadelphia: Lippincott Williams & Wilkins. xiii, 560, 45 p.
23. Benedict, S.H., et al., *Stereotactic body radiation therapy: the report of AAPM Task Group 101.* Med Phys, 2010. **37**(8): p. 4078-101.
24. Boujelbene, N., et al., *Stereotactic body radiation therapy in stage I inoperable lung cancer: from palliative to curative options.* Swiss Med Wkly, 2013. **143**: p. w13780.
25. Jang, S.S., et al., *The impact of respiratory gating on lung dosimetry in stereotactic body radiotherapy for lung cancer.* Phys Med, 2014. **30**(6): p. 682-9.
26. Underberg, R.W., et al., *Benefit of respiration-gated stereotactic radiotherapy for stage I lung cancer: an analysis of 4DCT datasets.* Int J Radiat Oncol Biol Phys, 2005. **62**(2): p. 554-60.
27. Li XA, K.P., Orton CJ, *Point/counterpoint. Respiratory gating for radiation therapy is not ready for prime time.* Med Phys, 2007. **34**: p. 867-70.
28. George, R., et al., *The application of the sinusoidal model to lung cancer patient respiratory motion.* Med Phys, 2005. **32**(9): p. 2850-61.
29. Lujan, A.E., et al., *A method for incorporating organ motion due to breathing into 3D dose calculations.* Med Phys, 1999. **26**(5): p. 715-20.
30. Bortfeld, T., et al., *Effects of intra-fraction motion on IMRT dose delivery: statistical analysis and simulation.* Phys Med Biol, 2002. **47**(13): p. 2203-20.
31. Lax, I., et al., *Dose distributions in SBRT of lung tumors: Comparison between two different treatment planning algorithms and Monte-Carlo simulation including breathing motions.* Acta Oncol, 2006. **45**(7): p. 978-88.
32. Guerrero, T., et al., *Elastic image mapping for 4-D dose estimation in thoracic radiotherapy.* Radiat Prot Dosimetry, 2005. **115**(1-4): p. 497-502.

www.manaraa.com

33. Ma, M., et al., *A Dosimetric Analysis of 3D Versus 4D Image-Based Dose Calculation for Stereotactic Body Radiation Therapy in Lung Tumors*, in *American Association of Physicists in Medicine Annual Meeting*. 2014, AAPM: Austin, TX.

34. Low, D.A., et al., *A technique for the quantitative evaluation of dose distributions.* Med Phys, 1998. **25**(5): p. 656-61.

35. Low, D.A. and J.F. Dempsey, *Evaluation of the gamma dose distribution comparison method.* Med Phys, 2003. **30**(9): p. 2455-64.

36. Muirhead, R., et al., *The potential clinical benefit of respiratory gated radiotherapy (RGRT) in non-small cell lung cancer (NSCLC).* Radiother Oncol, 2010. **95**(2): p. 172-7.

37. Lee, J.A., et al., *Four-dimensional computed tomography based respiratory-gated radiotherapy with respiratory guidance system: analysis of respiratory signals and dosimetric comparison.* Biomed Res Int, 2014. **2014**: p. 306021.

38. Berson, A.M., et al., *Clinical experience using respiratory gated radiation therapy: comparison of free-breathing and breath-hold techniques.* Int J Radiat Oncol Biol Phys, 2004. **60**(2): p. 419-26.

39. Linthout, N., et al., *Treatment delivery time optimization of respiratory gated radiation therapy by application of audio-visual feedback.* Radiother Oncol, 2009. **91**(3): p. 330-5.

40. Willoughby, T.R., et al., *Evaluation of an infrared camera and X-ray system using implanted fiducials in patients with lung tumors for gated radiation therapy.* Int J Radiat Oncol Biol Phys, 2006. **66**(2): p. 568-75.

41. Baker, R., et al., *Clinical and dosimetric predictors of radiation pneumonitis in a large series of patients treated with stereotactic body radiation therapy to the lung.* Int J Radiat Oncol Biol Phys, 2013. **85**(1): p. 190-5.

42. Barriger, R.B., et al., *A dose-volume analysis of radiation pneumonitis in non-small cell lung cancer patients treated with stereotactic body radiation therapy.* Int J Radiat Oncol Biol Phys, 2012. **82**(1): p. 457-62.

www.manaraa.com